1994

A Far-Ultraviolet Atlas of Symbiotic Stars Observed with IUE. I. the SWP Range

S. R. Meier
George Mason University

Menas Kafatos
Chapman University, kafatos@chapman.edu

R. P. Fahey
NASA, Goddard Space Flight Center

A. G. Michalitsianos
NASA, Goddard Space Flight Center

Recommended Citation

Meier, S.R., Kafatos, M., Fahey, R.P., Michalitsianos, A.G. (1994) A far-Ultraviolet Atlas of Symbiotic Stars Observed with IUE. I. the SWP Range, *Astrophysical Journal Supplement Series*, 94: 183-220. doi: 10.1086/192078

A Far-Ultraviolet Atlas of Symbiotic Stars Observed with IUE. I. the SWP Range

Comments

This article was originally published in *Astrophysical Journal Supplement Series*, volume 94, in 1994. DOI: 10.1086/192078

THE ASTROPHYSICAL JOURNAL SUPPLEMENT SERIES, 94:183–220, 1994 September

A FAR-ULTRAVIOLET ATLAS OF SYMBIOTIC STARS OBSERVED WITH *IUE*. I. THE SWP RANGE

S. R. MEIER[1] AND M. KAFATOS[2]
Department of Physics and CSI Institute, George Mason University, Fairfax, VA 22030
AND
R. P. FAHEY AND A. G. MICHALITSIANOS[2]
Laboratory for Astronomy and Solar Physics, NASA/Goddard Space Flight Center, Code 684.1, Greenbelt, MD 20771
Received 1993 January 26; accepted 1994 March 4

ABSTRACT

This atlas contains sample spectra from the far-ultraviolet observations of 32 symbiotic stars obtained with the *International Ultraviolet Explorer* (*IUE*) satellite. In all, 394 low-resolution spectra from the short-wavelength primary (SWP) camera covering the range 1200–2000 Å have been extracted from the *IUE* archive, calibrated, and measured. Absolute line fluxes and wavelengths for the prominent emission lines have been tabulated. Tables of both the general properties of these symbiotics and of features specific to the spectrum of each are included. The spectra shown are representative of the different classes of symbiotic stars that are currently in the *IUE* archive. These include known eclipsing systems and those that have been observed in outburst (as well as quiescence).

Subject headings: binaries: spectroscopic — line: identification — ultraviolet: stars

1. INTRODUCTION

Symbiotic stars are believed to be interacting binaries embedded in an ionized common envelope formed by a stellar wind lost by either one or both members of the system or by material that has been ejected during outbursts. Symbiotics generally consist of an M giant, which is often a Mira or late-type semiregular variable, and a hot companion with an effective surface temperature in the approximate range 25,000 K $\lesssim T_{\rm eff} \lesssim$ 100,000 K, appropriate to white dwarfs or the central stars of planetary nebulae. In a few cases, the presence of a main-sequence star is suspected. In many of these systems tidal interaction is believed to form an accretion disk around the compact secondary. The formation of hot accretion streams that results from the tidal interaction between the binary members may explain the presence of high-excitation permitted and intersystem emission lines that characterize symbiotics in the optical and UV.

Orbital periods of symbiotics vary from two to several dozen years. In these widely separated binaries, the stellar components evolve independently as long as both remain on the main-sequence, but they interact considerably during late stages of evolution. This particular evolutionary aspect uniquely distinguishes symbiotics from other classes of interacting binaries. The relevant interaction processes include mass expulsion from a common envelope between the stars, accretion disk formation, outbursts, and mass outflow that can lead to the formation of jetlike structures (e.g., CH Cyg, R Aqr). There is still much to learn about the nature of symbiotic systems due to the difficulty of directly observing the secondary star.

At visual wavelengths, symbiotic stars are characterized by the presence of absorption features and continua appropriate for a late-type M star, often a Mira or other long-period variable. Nebular emission lines, including both forbidden and Balmer line emission, suggest the presence of a high-excitation source (Boyarchuk 1975).

The near and far-UV afford an opportunity to directly probe the temporal behavior of high-excitation emission lines in symbiotics because the luminous M star, which dominates the integrated visible and infrared light, makes essentially no contribution at UV wavelengths. Thus, the far-UV provides a means of directly probing the high excitation source in these systems. The UV spectra of symbiotic stars suggest an enormous range of excitation that extends from low-temperature species such as O I λλ 1302–1306, C II λλ 1334,1335, Si II λλ 1806,1816, and Mg II λλ 2795,2802 to strong resonance emission lines such as N V λλ 1238,1242, C IV λλ 1548,1550, as well as other high-ionization lines such as He II λ1640 that are photoexcited by the EUV continuum radiation that corresponds to a source with a $T_{\rm eff}$ of at least 50,000 K to 100,000 K. Moreover, the intersystem lines of O IV] λλ 1397–1407, N IV] λ1487, O III] λλ 1660,1666, N III] λλ 1747–1753, Si III] λ1892 and C III] λλ 1907,1909 reflect the circumstellar nebular conditions of symbiotic stars.

Allen (1982) has defined two categories of symbiotic stars based upon IR photometry. Type S stars have blackbody continuum emission in the *K*-band, while type D symbiotics exhibit thermal silicate emission from dust. Most known symbiotics (∼110 out of 140) are S types, and about 30 (20%) are classified as type D.

S-type systems contain an M giant and often exhibit a stellar blackbody continuum flux distribution in the far-UV. In the 1200–2000 Å wavelength range of the *IUE* SWP camera this flux is generally appropriate to a $T_{\rm eff} \gtrsim$ 50,000 K star (Penston & Allen 1985), which is in agreement with the presence of the N V, C IV, and He II emission lines. The presence of strong silicate emission at 10 to 20 μm seems to correlate with the presence of long-period variables, e.g., Miras, in D-type symbi-

[1] University of Southern California, Space Sciences Center, Stauffer Hall of Science 274, Los Angeles, CA 90089.
[2] *IUE* Guest Observer.

otics (Allen 1982; Kafatos, Michalitsianos, & Feibelman 1982). The D-type symbiotics all have a similar UV continuum flux distribution (Penston et al. 1983) that rises with increasing wavelength in the 2000–3200 Å wavelength range of the *IUE* LWR/LWP cameras (see Kafatos, Michalitsianos, & Feibelman 1982). Since no hot secondary star has been directly observed in these systems, some secondary stars may be buried in the nebular material. Thermal IR emission, presumably from dust, may be associated with extensive mass loss from Mira winds.

The six known symbiotic stars positively identified with soft X-ray emission are: V1016 Cyg, RR Tel, HM Sge (Allen 1981), AG Dra, CH Cyg (Anderson et al. 1981) and R Aqr (Viotti et al. 1987). Four of these are D type. Accretion in the D-type systems may occur at rates as high as 10^{-5} or 10^{-4} $M_{\odot}$ yr^{-1}. These rates are higher than for the two S-type systems (AG Dra and CH Cyg), in which an inner accretion region with $T \sim 10^6$ K can explain the observed soft X-ray emission. Although it contains an M giant, the S-type symbiotic CH Cyg is a strong X-ray source. The other S-type, AG Dra, contains a K giant of ambivalent spectral class.

2. DESCRIPTION OF THE ATLAS

This atlas contains samples and analysis of the far-UV spectra of 32 symbiotic stars made with the *IUE* SWP camera between 1978–1988. We have selected the spectra with the best signal-to-noise ratio from those presently available in the *IUE* archive. Tracings of the spectra of 32 symbiotics are reproduced in Figures 1–32. In all, 394 low-resolution spectra with $\Delta\lambda \sim 6$ Å limiting resolution were examined, all in the 1200–2000 Å range. Part 2 of the atlas will present the spectra of symbiotics observed in the LWR/LWP wavelength range of 1900–3200 Å. A complete catalog of all 42 symbiotic stars that have been observed by *IUE* was not possible because many of the spectra were either significantly underexposed or saturated. This atlas complements various other catalogs (see Allen 1984; Sahade, Brandi, & Fontenla 1984; Kenyon 1986).

Table 1 lists the observational parameters for each object: right ascension, declination, date and time, SWP number, and, if applicable, orbital phase. A final column indicates whether an eruptive object was in the active or quiescent stage. The absolute line intensities for the most prominent emission lines present in the SWP wavelength range are shown in Table 2. Several of the symbiotic stars in the Atlas have far-UV spectra that show large temporal flux variations. These include both systems with phase-dependent occultation effects in known eclipsing binaries with well-determined ephemerides and outburst systems in active and in quiescent states.

General properties of the stars in the atlas, such as spectral type, radio flux, Mira period, etc., are given in Table 3. Finally, Table 4 compares the spectral features such as intercombination line strength, resonance line strength, and continuum flux distribution of the symbiotic stars.

3. OBSERVATIONS AND ANALYSIS

The *IUE* spectra presented in the atlas were analyzed and produced with data analysis routines written in IDL available at the *IUE* Regional Data Analysis Facility (RDAF) at the NASA Goddard Space Flight Center. Since the *IUE* spectra presented in this atlas were collected at different epochs, we have reprocessed all of the *IUE* SWP spectra with the latest IUESIPS data reduction routines. This insures, as much as possible, that all spectra for each object have been analyzed using the same calibration and extraction procedures.

For objects that exhibit strong UV flux variations, i.e., eclipsing systems and systems with active and quiescent states, we have given the absolute fluxes at the phases specified in Table 1. For the faintest stars (BI Cru, LMC Anon, He 2-38), spectra have been co-added to increase the signal-to-noise ratio. The spectra in this atlas have not been corrected for interstellar extinction, because the precise nature and value of the circumstellar extinction component present is quite uncertain. However, accepted values for E_{B-V} are listed in Table 3.

In systems where the UV continuum is well exposed, absolute emission-line fluxes are taken relative to the continuum base. Otherwise, in weak continuum objects the absolute fluxes are taken above zero. The absolute emission-line fluxes found in Table 2 are subject to *IUE* uncertainties of about 20% for the strongest lines. The weaker lines are more affected by calibration errors and poor signal-to-noise ratio. In addition, there has been a mean sensitivity degradation in the SWP camera of about 1% per year (Bohlin & Grillmair 1988). Combining these effects, we estimate a maximum uncertainty in the comparison of absolute *IUE* line fluxes of approximately 30% over the period from 1978 to 1988.

4. DISCUSSION OF INDIVIDUAL STARS

In this section we provide brief descriptions of the far-UV spectra and the most important properties of the symbiotic stars in this atlas. Further information about each of these objects is provided in the accompanying tables.

4.1. *EG Andromedae*

We present in Figure 1 UV spectra of EG And both in and out of eclipse during the years 1978–1984. The spectra shown illustrate its behavior at visual minimum and maximum phases (Chochol et al. 1987). Principal among the emission lines in the far-UV are N IV], C IV, He II, O III], N III], Si III], and C III]. The continuum flux distribution clearly increases toward shorter wavelengths out of eclipse yet vanishes when the star is near minimum phase. This could indicate that the hot star is being eclipsed by the extended atmosphere of the cool primary (see Fig. 1). Several emission lines (e.g., N V λλ 1238,1242, O I λλ 1302–1306, He II λ1640, and N IV λ1718) are very weak at minimum phase. Using a UV light curve, on the other hand, Munari et al. (1988) explain these variations as a reflection effect rather than eclipse-like variations of the star. We suggest that these variations could also occur if the high-excitation lines N V λλ 1238,1242 and He II λ1640 are formed close to the secondary star, in which a high-excitation, compact line-emitting region is more susceptible to eclipses.

4.2. *AX Persei*

Figure 2 shows UV spectra of AX Per corresponding to several orbital phases in the visible. For this, we used the optical ephemeris determined by Kenyon (1982). The UV continuum flux distribution is flat during optical minimum but increases

TABLE 1

IUE OBSERVATIONS OF SELECTED SYMBIOTIC STARS IN THE FAR-ULTRAVIOLET

Object	α (1950.0)	δ (1950.0)	Julian Date (244+)	SWP Image No.	Exposure Time (min.)	Exposure Start Time (UT)	Orbital Phase	Activity/ Quiescence
EG And	$00^h\ 41^m\ 52.7^s$	40° 24′ 22″	3873	3753	50	$21^h\ 34^m$	0.80	
			4072	5834	60	14 45	0.22	
			4451	9644	12	16 17	0.03	
			4614	11007	30	05 24	0.37	
			4894	15273	15	11 28	0.96	
			5272	18424	15	12 44	0.75	
			5386	19303	15	00 10	0.99	
			5537	20497	10	15 15	0.31	
			5748	22285	15	03 24	0.76	
			5976	24097	15	05 56	0.24	
AX Per	01 33 06.0	54 00 18	3874	3755	50	03 40	0.56	
			4119	6360	40	13 17	0.91	
			4156	6808	10	18 06	0.97	
			4614	11008	45	07 02	0.64	
			4831	14758	10	16 07	0.96	
			5532	20479	40	22 00	0.99	
			5894	23448	15	14 01	0.52	
			6111	25244	15	20 07	0.84	
LMC Anon	05 46 02.7	-71 17 13	5261	18315	295	00 56		
			6248	26327	425	05 03		
			7396	34122	342	23 26		
LMC S63	05 48 52.4	-67 37 02	5050	16591	240	11 35		
RX Pup	08 12 28.2	-41 33 18	4504	10189	45	02 47		
			4767	14239	15	14 52		
			5051	16598	15	16 38		
			5638	21403	15	05 29		
			5771	22462	15	18 34		
			6560	28284	12	21 05		
He2-38	09 53 03.7	-57 04 39	4831	14752	15	02 33		
			5908	23517	60	11 45		
SY Mus	11 29 55.0	-65 08 36	4503	10188	90	23 47	0.88	
			4767	14237	45	11 33	0.30	
			4939	15594	60	00 42	0.57	
			4950	15705	9	02 26	0.59	
			5020	16381	60	18 11	0.70	
			5834	23011	90	15 22	0.00	
BI Cru	12 20 40.3	-62 21 39	4690	13583	60	14 52		
			4939	15595	95	02 17		
RW Hya	13 31 32.0	-25 07 29	3876	3779	18	07 28		
			4074	5863	10	18 22		
			4451	9645	30	17 44		
			4613	11000	10	17 20		
			6238	26220	5	16 21		
			6940	31038	8	20 31		
He2-106	14 10 22.7	-63 11 45	5908	23515	70	04 37		
Hen-1092	15 42 29.9	-66 19 59	4300	8096	40	06 28		

TABLE 1—*Continued*

Object	α (1950.0)	δ (1950.0)	Julian Date (244+)	SWP Image No.	Exposure Time (min.)	Exposure Start Time (UT)	Orbital Phase	Activity/ Quiescence
T CrB	15 57 24.5	26 03 39	3879	3815	25	18 59		
			4070	5804	80	07 14		
			5124	17104	55	03 05		
			6188	25834	45	04 26		
			6453	27556	50	11 18		
			6631	28715	35	20 56		
AG Dra	16 01 23.2	66 56 25	4054	5676	16	18 43		Quiescent
			4536	10456	25	09 03		Quiescent
			4613	11002	4	20 19		Active
			4692	13605	8	23 22		Active
			4820	14640	15	20 33		Active
			4950	15709	15	10 07		Active
			5499	20209	20	00 58		Quiescent
			5908	23520	18	16 48		Quiescent
			5916	23582	20	21 01		Quiescent
			6449	27542	10	14 18		Active
HK Sco	16 51 29.8	-30 18 16	4690	13582	75	11 19		
			5021	16392	120	17 21		
CL Sco	16 51 40.3	-30 32 30	4440	9543	60	13 15		
H1-36 Ara	17 46 24.1	-37 00 36	4157	6819	30	19 00		
Y CrA	18 10 47.3	-42 51 26	4157	6820	35	20 42		
YY Her	18 12 25.9	20 58 20	4385	9115	35	16 14		
			4464	9773	80	16 18		
			4943	15652	150	22 55		
AS 296	18 12 30.8	-00 19 53	5020	16380	60	14 45		
			5268	18389	55	12 54		
			7226	33047	145	16 24		
			7477	34725	40	13 44		
AS 295B	18 12 51.9	-30 52 16	4089	6063	105	23 13		
AR Pav	18 15 24.6	-66 06 07	4072	5829	10	07 09	0.27	
			4451	9646	25	18 57	0.90	
			4543	10510	60	22 45	0.05	
			4735	13956	50	20 50	0.37	
			5067	16710	30	11 46	0.91	
			5089	16857	100	11 41	0.95	
			5120	17070	90	09 04	0.99	
			5801	22707	55	06 10	0.13	
V443 Her	18 20 02.8	23 25 48	4385	9122	20	23 12		
			4534	10439	24	10 17		
BF Cyg	19 21 55.2	29 34 34	4054	5671	80	10 27	0.31	
			4344	8758	20	18 01	0.70	
			4677	13477	60	08 10	0.14	
			6634	28734	30	01 52	0.72	
			6922	30924	15	04 33	0.10	
			7302	33579	30	03 47	0.60	
CH Cyg	19 23 14.2	50 08 31	4223	7409	15	03 48		
			5720	22056	0.5	13 32		
			6089	24956	6	13 36		
			6238	26219	15	14 39		
			6333	26720	30	15 45		
			6454	27571	25	12 11		
			6627	28682	12	22 41		
			6817	30134	12	08 43		

TABLE 1—*Continued*

Object	α (1950.0)	δ (1950.0)	Julian Date (244+)	SWP Image No.	Exposure Time (min.)	Exposure Start Time (UT)	Orbital Phase	Activity/ Quiescence
HM Sge	19 39 41.4	16 37 33	4477	9898	25	18 29		
			4831	14756	45	11 50		
			5073	16752	15	03 01		
			6657	28896	11	18 54		
			6889	30694	92	02 42		
CI Cyg	19 48 21.0	35 33 24	4036	5485	45	05 42	0.57	
			4269	7818	60	21 30	0.85	
			4453	9663	25	15 53	0.06	
			4613	11003	40	22 38	0.25	
			4894	15274	20	13 28	0.58	
			5142	17276	15	15 30	0.87	
			5294	18603	15	02 53	0.04	
			5567	20731	16	17 33	0.36	
V1016 Cyg	19 55 19.8	39 41 30	3752	2427	40	22 36	0.90	
			3920	4271	30	22 48	0.95	
			4049	5611	20	22 32	0.99	
			4475	9878	20	18 34	0.11	
			5422	19566	25	04 15	0.38	
			6045	24656	25	10 50	0.56	
			6772	29829	25	10 47	0.77	
			7112	32296	25	16 20	0.87	
RR Tel	20 00 20.1	-55 52 04	3709	2047	2	03 09		
			4076	5885	6	19 40		
			4330	8610	1.25	07 46		
			6563	28292	3	00 03		
			6730	29536	3	19 42		
			6949	31080	3	02 10		
HBV 475	20 49 02.6	35 23 37	4477	9900	30	22 56	0.64	
			4825	14688	87	00 20	0.01	
			5074	16760	50	02 49	0.27	
			5423	19575	25	03 24	0.63	
			5816	22840	85	07 21	0.05	
			6354	26943	35	15 02	0.61	
			6770	29815	70	10 08	0.05	
			7430	34313	40	17 59	0.75	
AG Peg	21 48 36.2	12 23 27	3720	2123	2	14 52		
			3878	3795	8	00 23		
			4119	6354	6	01 49		
			4385	9117	3	18 20		
			4536	10455	3	08 20		
			6213	26023	5	17 40		
Z And	23 31 15.3	48 32 32	4070	5809	15	20 25		Quiescent
			4614	11006	40	03 51		Quiescent
			6353	26937	60	18 41		Active
			6374	27028	35	12 04		Active
			6402	27203	7	04 40		Active
			6461	27632	8	09 50		Active
			7101	32208	22	18 25		Quiescent
			7195	32845	30	10 29		Quiescent
R Aqr	23 41 14.3	-15 33 42	3877	3792	42	19 10		
			4074	5856	10	08 20		
			5097	16918	30	15 44		
			5480	20069	40	13 30		
			6286	26569	45	09 52		
			6617	28611	45	09 34		
			6736	29562	120	01 23		
			7162	32646	40	23 17		

1994ApJS...94..183M

TABLE 2

FLUXES OF THE SYMBIOTICS OBSERVED BY *IUE*

Star	N V	Si II	O I	C II	Si IV	O IV]	N IV]	C IV	[Ne V]	[Ne IV]	He II	O III]	N IV	N III]	Si II	Si III]	C III]
	1238.8 1242.8	1264.9	1301.1 1304.9	1334.5 1335.7	1393.8	1397.2 1399.8 1401.1 1404.8	1483.3 1486.5	1548.2 1550.8	1574.7	1601.5	1640.4	1660.8 1666.1	1718.5	1746.8 1748.6 1749.6 1752.1 1753.9	1808.0 1816.9 1817.4	1892.0	1906.7 1908.7
EG And																	
SWP	1240.0	1266.5	1304.2	1334.5	1394.7	1401.3	1486.0	1548.4	1576.0	1600.2	1639.6	1663.6	1717.8	1750.2	1815.4	1891.7	1908.1
3753	216.6	60.3			*423.7	*507.1	*601.4	*2051.0			259.1	*836.1	21.5	*303.4	29.3	*191.8	*475.2
5834	*149.5	78.9	*119.6		*294.4	*391.8	*482.1	*1170.0			*302.9	*623.1	156.7	*208.9		*167.0	*222.1
9644	41.6				484.1	422.2	528.0	*4711.0		18.2	372.7	1016.0	34.7	243.0		132.8	563.9
11007	*364.3	106.0	*788.2	16.1	*641.6	*741.5	*743.6	*2545.0	24.0		*687.3	*1343.0	113.3	*434.1	118.1	397.5	*678.9
15273	25.6				505.3	398.1	126.3	*2801.0			41.9	659.9		273.9	16.7	165.2	710.3
18424	139.9		219.0		309.4	364.9	877.4	*4298.0			320.8	*1886.0	78.9	397.9	12.1	376.1	951.2
19303					344.7	229.0	327.5	*3649.0			24.2	*787.7		192.1	12.5	160.2	*633.0
20497	220.0		616.7		606.6	851.9	1122.0	*5351.0			416.9	2195.0	332.4	496.5		441.1	1185.0
22285	233.2	87.7	217.4		499.2	634.1	942.8	*4713.0	21.1		329.3	*1895.0	82.5	418.9	49.1	347.9	*918.8
24097	251.1	56.6	76.6		256.4	445.6	858.9	*3996.0	36.9		412.8	*1699.0	59.5	319.5		290.1	*876.8
AX Per																	
SWP	1239.6	......	1303.4	1331.6	1395.1	1402.3	1486.2	1548.8	1575.5	1601.2	1640.0	1664.5	1720.3	1750.3	1817.2	1892.7	1908.5
3755	171.2		98.4	8.2	140.9	268.2	350.1	*1285.0		4.5	*477.8	*746.2	28.7	*363.2	38.0	*308.2	*608.0
6360	105.1				88.1	130.0	161.8	*1072.0		12.2	188.9	317.2	11.1	187.3	9.9	84.9	*464.7
6808	67.2				88.1	95.5	136.7	1072.0			129.4	319.1		156.6		68.7	491.1
11008	261.7		119.8		124.5	277.7	344.6	*1117.0	35.9	30.5	*527.8	*517.5	40.2	186.3	33.7	155.8	*352.9
14758	261.1				61.1	178.2	196.1	1272.0	80.7	49.2	496.0	185.2		112.3		24.7	155.2
20479	126.9				43.8	101.0	86.9	610.7	12.7	16.2	273.3	112.7	9.9	48.5		35.8	113.5
23448	345.1		129.1		159.0	220.0	253.7	1964.0	25.8	17.2	515.6	508.9	33.4	143.0	21.1	134.8	208.4
25244	111.9				39.2	114.1	125.4	834.4			348.4	179.2		107.0	25.1	18.6	137.4
LMC Anon																	
SWP	1239.4	.....	1303.0	.....	.....	.....	1485.8	1548.7	.....	.....	1640.4	1663.1	1722.6	1750.8	.....	1896.7	1904.9
18315	29.1						12.6	4.3			6.8	2.4	2.1	11.0			
26327	22.9		2.1				12.7	7.7			5.6	4.4		12.2			
34122	20.2						13.3	5.4			3.7	1.6		10.7		0.6	1.3
LMC S63																	
SWP	1245.9	1268.6	....	1333.7	1397.3	1404.7	1488.6	1552.9	.....	....	1643.2	1665.1	1722.8	1752.5	1819.5	1894.9	1911.8
16591	12.9	3.1		2.4	2.4	4.1	18.1	61.2			20.6	14.3	3.0	9.3	1.9	2.1	36.9

TABLE 2—*Continued*

	N V	Si II	O I	C II	Si IV	O IV]	N IV]	C IV	[Ne V]	[Ne IV]	He II	O III]	N IV	N III]	Si II	Si III]	C III]
RX Pup																	
SWP	*1239.9*	.....	*1304.6*	*1337.9*	*1395.4*	*1403.0*	*1486.3*	*1549.7*	*1574.3*	*1601.5*	*1640.5*	*1665.1*	*1716.6*	*1751.0*	*1817.0*	*1892.5*	*1909.0*
10189	7.8		80.2	5.2	116.7	135.0	282.5	*1008.0			458.1	*582.4	35.4	*346.1	55.5	*336.1	*557.9
14239	27.5		99.5		91.6	161.8	344.1	1185.0	26.1	24.1	539.1	591.2		380.8	44.8	419.0	*987.5
16598	40.4		129.6		45.4	162.7	344.1	1171.0	25.2	17.2	586.9	520.9	11.0	349.4	28.8	330.4	*980.1
21403	76.3		21.2		115.6	207.7	309.2	921.5		25.1	600.9	397.5	9.1	251.0	28.1	276.3	*831.6
22462	79.5		23.0	26.9	97.6	226.7	341.2	900.7			550.4	345.4	50.9	223.1	26.9	218.9	*820.9
28284	115.4		35.1		141.1	250.6	287.9	912.4			501.0	283.6		203.4	42.1	121.5	560.4
He2-38																	
SWP	*1240.7*	.....	.....	.....	*1396.6*	*1404.2*	*1488.2*	*1550.3*	.....	*1598.8*	*1641.2*	*1666.0*	.....	*1750.4*	*1819.4*	*1896.5*	*1910.6*
14752	23.1					5.9	4.8	154.4		10.5	48.1	38.9		17.0	5.9	8.2	62.1
23517	7.4				2.0	4.8	5.9	104.2			13.9	14.3		9.1		12.3	35.6
SY Mus																	
SWP	*1239.6*	*1263.3*	*1304.5*	.....	*1395.3*	*1401.8*	*1486.3*	*1548.7*	*1574.8*	*1601.5*	*1640.1*	*1664.5*	*1718.5*	*1750.9*	*1817.7*	*1890.9*	*1909.0*
10188	114.0		7.7		78.7	158.0	88.2	*560.0	24.1		*439.6	97.0	2.9	63.2	60.7	88.3	
14237	*1089.0		252.2		*385.0	*663.6	410.3	*1822.0	50.2	9.8	*980.3	427.2	33.9	151.2	21.9	188.3	145.4
15594	*1003.0	20.4	254.7		*374.5	*554.5	*367.9	*1505.0	33.6		*882.0	459.2	11.0	150.5	29.5	*207.7	146.7
15705	1106.0		247.8		328.8	523.1	351.7	*3342.0		11.0	1569.0	468.0		138.8	31.9	204.3	163.7
16381	*709.0		121.1		*213.6	*418.0	254.8	*1236.0	21.5	11.5	*706.9	311.1	10.0	118.5	7.9	124.3	113.3
23011	91.5		10.8		54.0	137.0	78.1	*473.6	22.5	4.9	*440.5	101.0	13.5	49.3		30.0	72.8
BI Cru																	
SWP	*1239.4*	.....	.....	*1335.0*	*1396.8*	*1405.8*	.....	.....	.....	.....	*1641.7*	*1662.4*	*1718.2*	*1755.4*	*1816.2*	*1896.4*	*1909.7*
13583	6.0					5.1					4.1	5.5	1.4	3.0		2.4	4.4
15595	6.1			3.6	3.7						2.1	10.9		5.7	2.1	12.1	
RW Hya																	
SWP	*1239.7*	*1266.1*	*1305.7*	......	*1395.0*	*1401.9*	*1486.4*	*1548.6*	*1576.9*	*1601.0*	*1640.7*	*1664.2*	*1719.2*	*1750.3*	*1815.6*	*1891.6*	*1909.5*
3779	1027.0	121.4	185.5			*3650.0	*2987.0	*7776.0			*1572.0	*2589.0	69.9	423.9	67.6	251.6	422.2
5863	719.7	496.2	653.2		1714.0	*4950.0	*4070.0	*10840.0			*2326.0	*3696.0	222.2	462.2	71.0	394.9	498.7
9645	*95.9	*222.4	*186.8			*1295.0	*1821.0	*5170.0	54.6	38.9	*822.6	*1070.0		282.1	57.7	214.7	305.3
11000	1446.0	194.4	67.1			*4637.0	*3744.0	*10970.0		41.9	*1497.0	*3008.0	63.2	360.6	31.0	185.5	391.6
26220	1194.0					*4259.0	*3130.0	*10580.	56.9		1203.0	2227.0	49.7	331.9		168.4	298.9
31038	330.1	21.4	33.4			*1692.0	1429.0	*7807.0		75.8	725.1	1136.0		98.7	54.9	92.5	265.5
He2-106																	
SWP	*1242.6*	.....	*1303.3*	.....	.....	.....	*1487.7*	*1550.5*	....	.....	*1641.1*	*1665.1*	.....	.....	*1817.6*	*1893.0*	*1912.7*
23515	4.6		1.8				5.3	23.2			15.0	15.4			1.0	1.4	4.5

1994ApJS...94..183M

TABLE 2—*Continued*

	N V	Si II	O I	C II	Si IV	O IV]	N IV]	C IV	[Ne V]	[Ne IV]	He II	O III]	N IV	N III]	Si II	Si III]	C III]
Hen 1092																	
SWP	1238.9	.....	1304.3	1337.3	1393.7	1401.1	1485.7	1548.1	1574.0	.....	1639.3	1663.1	1719.3	1749.0	1817.2	1890.2	1908.5
8096	99.2		30.5	3.5	44.9	13.1	83.1	413.0	23.9		383.8	142.7	8.1	18.4	4.5	21.1	34.4
T CrB																	
SWP	1239.6	1264.5	1305.5	1337.0	1391.4	1400.8	1486.6	1547.8	1577.4	1599.7	1640.6	1665.7	1714.4	1751.1	1817.3	1891.7	1909.9
3815	135.3		80.6			18.9	38.0	334.3		26.1	83.0	39.3	9.8	158.5	21.1	104.9	86.0
5804	28.1	6.2	49.9			26.2	22.3	158.1			63.5	38.7		60.2	8.4	70.9	38.4
17104	117.2		102.6	14.0	83.7	79.9	76.1	492.8			129.8	82.6	11.7	154.8		165.0	137.0
25834	281.9		172.6	19.6	140.2	110.1	108.0	463.9	51.4		156.3	95.3		158.8	12.1	186.7	148.3
27556	99.6		73.3		100.6	84.3	35.1	333.1			61.0	59.3		94.2		113.9	80.5
28715	48.4		36.1	7.7		51.2	37.1	82.1			20.7	22.5		31.7		30.8	42.9
AG Dra																	
Active																	
SWP	1239.0	1264.9	1304.3	.....	1393.5	1401.1	1485.7	1548.5	1576.7	.....	1639.1	1664.5	1718.4	1749.4	1817.9	1892.0	1910.5
11002	2443.0				582.5	1477.0	533.7	3903.0	88.6		*9840.0	331.3		306.3			215.5
13605	*2933.0		211.4		724.0	1927.0	492.1	*3759.0			*6096.0	533.9	65.8	85.4		239.0	130.2
14640	*2689.0	185.2	320.3		*438.2	*1282.0	571.4	*2632.0	78.9		*3513.0	502.1		53.2		270.0	64.9
15709	*947.2				*123.2	*437.6	*254.0	*1608.0			*2454.0	*85.7					
27542	*3359.0		219.1			2149.0	658.8	*3905.0			*6990.0	324.0	49.6		45.6	141.1	22.9
Quiescent																	
	1239	1266	1303.8	.....	1395.2	1401.4	1486	1548.2	1575.8	1602.8	1639.5	1664.1	1715.8	1750.9	1817.7	1891.2	1910.4
5676	*590.8		80.1		97.1	446.7	174.9	609.9	50.2		*1806.0	104.4				92.3	32.7
10456	*906.4	22.8	111.4		173.3	559.8	195.5	953.8			*2172.0	234.1		51.7		96.9	37.0
20209	*1448.0		171.3		332.0	653.2	252.3	1286.0	28.2	31.6	*2389.0	207.6	32.6	71.3	18.9	89.2	25.2
23520	548.9		95.1			345.9	125.5	376.4			*1453.0	130.7		51.4		23.1	
23582	476.7		51.9		117.9	324.3	135.8	479.1			*1447.0	109.7	39.0	16.5		49.3	
HK Sco																	
SWP	1239.1	.....	1302.8	1337.3	1393.3	1403.6	1490.3	1548.5	1577.2	.....	1640.2	1663.5	.....	1750.1	1819.7	1893.1	1910.8
13582	17.3		6.9	5.5	6.3	19.6	19.0	110.7	6.1		74.7	18.1		8.1	4.1		5.6
16392	28.6		1.3			8.3	6.9	30.0	4.2		35.2	8.6		2.4	2.4	3.5	5.0
CL Sco																	
SWP	....	.....	1303.9	1338.3	1395.3	1404.1	1485.5	1550.8	....	.....	1639.1	1664.6	....	.....	......	1891.7	1909.1
9543			16.3	6.4	8.9	4.0	5.2	55.9			24.0	68.1				59.7	104.6
H1-36 Arae																	
SWP	.....	......	1300.6	....	.....	1404.5	1491.8	1547.1	.....	.....	1638.1	1663.0	.....	1747.4	1815.3	.....	1907.0
6819			3.1			3.0	11.2	40.1			17.3	1.9		17.3	1.9		45.6
Y CrA																	
SWP	1239.4	.....	1305.9	1335.5	......	1401.9	1487.4		1576.1	1598.9	1639.5	1663.6	1720.6	1748.1	1815.3	1891.3	1908.5
6820	73.0		15.3	2.1		88.1	60.3		16.5	9.7	247.4	105.9	5.0	39.0	5.1	22.8	81.8

TABLE 2—*Continued*

	N V	Si II	O I	C II	Si IV	O IV]	N IV]	C IV	[Ne V]	[Ne IV]	He II	O III]	N IV	N III]	Si II	Si III]	C III]
YY Her																	
SWP	1240.0	1265.8	1305.0	.....	1395.4	1402.2	1486.4	1549.4	1575.9	1602.0	1640.3	1664.1	1719.0	1749.8	1816.1	1891.7	1908.7
9115	153.0		53.3			291.6	291.1	392.5	20.9		391.6	390.0		55.8	9.8	38.9	95.4
9773	186.3		45.8			157.7	142.9	287.2	11.7	8.2	*260.3	220.5	12.7	30.5	3.9	28.4	48.8
15652	20.2	1.9	14.2		24.6	75.4	67.7	168.3	5.8	5.5	*115.9	*180.3		46.1	5.7	*38.4	*106.2
AS 296																	
SWP	1238.8	......	1305.7	.....	1396.8	1405.2	1484.6	1549.3	1576.6	1603.2	1639.9	1665.2	1720.2	1750.7	1819.0	1893.9	1910.5
16380	16.1				14.0		20.2	229.4	1.9	5.6	25.9	43.6	8.6	16.2	1.6	7.9	10.2
18389					4.5	6.7	53.3	52.6			11.6	13.4		11.2	7.7	2.7	3.6
33047					5.6	12.1	12.1	120.0			20.2	16.8	3.4	15.5	0.6	1.4	10.3
34725			3.8		3.8	5.3		52.6				58.1		22.2	3.5	19.2	37.5
AS 295B																	
SWP	1239.5	....	1304.2	....	1396.0	1404.3	1487.8	1546.6	1575.9	....	1641.0	1659.9	1721.2	1747.6	.....	1892.0	1911.0
6063	9.6		4.3		1.3	4.4	9.8	24.1	2.6		22.3	2.2	1.8	12.6		8.0	2.3
AR Pav																	
SWP	1240.9	1266.6	1306.0	1334.6	1395.2	1402.4	1486.9	1549.3	1577.6	1602.5	1640.6	1664.6	1717.4	1751.0	1814.9	1891.8	1908.7
5829	133.2	25.6	58.0	46.0	170.5	282.1	272.6	1579.0	24.6		425.9	960.8		309.4		203.7	922.9
9646	108.5	12.7	86.2	15.2	102.1	144.6	111.8	641.1	40.4		195.0	307.8		125.9		193.3	365.5
10510	152.2		52.5	7.2	86.5	140.4	93.3	*661.9	4.5	19.9	186.9	290.3		100.7	16.6	112.5	*317.4
13956	121.1	9.7	45.6		113.4	300.0	240.7	*933.7	10.4		*457.0	*612.1		182.0	6.4	*185.7	*421.1
16710	118.6		57.6		121.5	196.5	158.7	679.7			257.7	449.7		122.5		112.9	452.5
16857	121.2		44.7		88.0	171.7	134.9	*635.9	5.8	11.6	188.0	*380.8		124.6	17.3	*133.1	*318.9
17070	120.2		34.9		87.6	140.8	116.2	*619.2	8.5	6.8	145.5	*349.6	9.1	103.7	10.4	120.8	*349.4
22707	85.4		27.7		110.7	215.9	107.3	*974.3			297.3	488.1		136.7	23.8	197.4	*370.4
V443 Her																	
SWP	1240.5	.....	1304.1	....	1394.4	1400.5	1485.1	1547.5	1575.8	1600.5	1638.6	1662.6	....	1749.0	1813.6	1890.2	1907.0
9122	188.6		126.5		253.7	643.3	815.8	*2682.0		83.4	387.0	953.5		254.9		112.4	381.0
10439	210.7		143.3		267.8	756.3	*852.3	*2961.0	56.9	61.9	506.7	*1239.0		262.8	27.9	154.4	443.2
BF Cyg																	
SWP	1243.6	1265.2	1305.2	.....	1393.8	1402.9	1486.3	1550.4	1573.8	1602.5	1640.3	1664.0	1720.6	1750.0	1816.6	1891.5	1907.8
5671	153.4	32.0	84.4		*78.7	68.6	55.3	*410.5			*164.9	*339.1	45.6	*264.8	16.7	*210.7	*307.6
8758	158.6		43.0		171.5	166.7	176.3	863.2		36.9	144.6	624.9	43.4	419.3	37.8	185.4	*671.3
13477	15.4				63.9	76.2	90.1	*735.9			70.2	264.6	30.9	*230.1		74.8	*351.8
28734	141.1	36.2	304.0		288.2	163.6	108.0	686.2			178.2	956.7	52.4	*733.0	17.7	368.9	*856.7
30924	15.9		23.1	3.4	176.5	127.1	29.6	649.0	44.6	21.1	45.0	383.1		369.0		289.9	722.0
33579	213.4	36.2	416.7	3.5	265.4	237.2	187.8	*937.8	27.9	34.1	140.1	*1118.0	29.4	*846.6	45.2	*540.8	*1127.0

TABLE 2—*Continued*

	N V	Si II	O I	C II	Si IV	O IV]	N IV]	C IV	[Ne V]	[Ne IV]	He II	O III]	N IV	N III]	Si II	Si III]	C III]
CH Cyg																	
SWP	*1242.4*	*1264.0*	*1306.3*	*1336.3*	*1394.1*	*1403.7*	*1489.7*	*1548.1*	*1578.1*	*1603.1*	*1642.2*	*1667.0*	*1713.8*	*1749.1*	*1817.6*	*1892.1*	*1909.8*
7409			*1426.0		358.2	97.3	790.3	513.6			532.5	662.0	*148.8			*165.4	*217.1
22056	1723.0		1478.0		1683.0		3008.0	2848.0			5315.0	1971.0	1486.0	1469.0		5750.0	1079.0
24956	1300.0	380.6	3573.0	913.4	364.5	647.5	521.5	1673.0			1689.0	508.6	173.3	1538.0	782.1	1323.0	1608.0
26219	844.9	287.5	*2128.0	656.0	447.6	687.1	342.5	*2229.0	80.5	80.2	731.3	650.4		832.9	21.2	*1060.0	*1063.0
26720	632.2	339.2	*1594.0	656.9	406.8	622.0	236.1	1647.0			641.8	516.7		624.3	*291.6	*799.1	*947.8
27571	472.7	169.5	*1300.0	*588.1	478.5	584.4	209.4	*2038.0			*915.6	*812.1	142.3	*668.0		*630.6	*673.8
28682	339.6	48.7	885.9	313.0	1039.0	945.7	959.9	*3072.0			729.8	1010.0	*109.8	*733.9		*1076.0	*979.6
30134	153.0	25.8	314.0	256.4	447.3	409.4	168.3	1426.0			291.4	411.1	44.5	332.2	137.3	519.3	592.7
HM Sge																	
SWP	*1240.3*	*1263.2*	*1303.1*	*1335.4*	*1396.6*	*1401.8*	*1486.0*	*1549.1*	*1576.1*	*1601.0*	*1640.1*	*1664.4*	*1717.3*	*1750.7*	*1816.5*	*1893.7*	*1908.3*
9898	235.8		10.8	19.1	112.5	200.0	428.9	*1336.0	30.9	88.8	583.5	263.0	6.2	332.5	33.4	291.6	*928.3
14756	335.3			20.3	92.5	216.7	*509.4	*1164.0	38.1	131.8	*597.3	297.6		*362.3	39.5	316.5	*627.7
16752	252.8		11.2	19.7	140.3	256.0	538.1	1613.0	14.4	111.4	785.0	374.0	18.3	355.8	37.7	317.3	*1157.0
28896	406.4					383.3	491.5	2045.0	41.9	97.4	1084.0	254.9		344.7	46.1	185.9	1033.0
30694	*452.8	3.2	6.0	11.9		*477.0	*512.1	*1032.0	52.4	117.8	*634.9	232.4	11.1	*309.4	33.7	*99.8	*498.1
CI Cyg																	
Active																	
SWP	*1240.0*	.....	*1304.1*	*1335.1*	*1395.3*	*1402.6*	*1486.6*	*1549.1*	*1577.3*	*1601.6*	*1640.4*	*1664.6*	*1720.3*	*1750.9*	*1815.6*	*1892.5*	*1908.7*
5485	153.7		78.3		110.0	159.1	314.8	*1254.0	12.8	24.6	272.4	498.4		356.0	38.3	197.3	*595.7
7818	162.5		23.1		131.4	220.4	318.8	*1158.0	20.7	27.1	*373.6	*462.5	16.3	*302.8	12.3	146.8	*452.6
9663	130.3		16.5	13.2	131.6	159.2	225.7	*1339.0	16.5	8.1	274.9	393.1	9.3	256.9		157.5	*575.5
11003	238.8		20.2	3.6		249.2	329.2	*995.4	28.3	39.2	497.2	*380.1	28.8	208.0	20.6	163.0	*446.9
Quiescent																	
	1239.8	*1264.7*	*1302.7*	*1336.3*	*1395.6*	*1402.3*	*1486.6*	*1549.6*	*1575.4*	*1601.8*	*1640.7*	*1665.1*	*1719.2*	*1750.9*	*1817.9*	*1892.9*	*1909.9*
15274	222.5		91.3		85.3	226.0	307.4	1039.0	23.2	25.3	510.2	328.6		171.9	16.5	186.6	395.7
17276	183.6		22.1	16.5	113.9	222.5	233.0	1203.0	21.8	18.3	576.6	267.7		147.9	15.5	110.0	340.9
18603	192.6	14.0	7.3		54.5	139.2	174.8	1230.0	26.3	17.2	404.5	203.8	9.4	115.9	6.7	41.7	283.6
20731	671.8	23.0	229.7		156.1	366.9	332.9	*2657.0	84.9	39.0	990.3	373.2	20.4	168.6	54.9	183.3	262.1
V1016 Cyg																	
SWP	*1239.8*	*1265.7*	*1305.0*	*1336.4*	*1396.1*	*1401.7*	*1486.3*	*1548.7*	*1574.5*	*1601.2*	*1639.9*	*1664.1*	*1718.3*	*1750.5*	*1816.7*	*1892.4*	*1907.4*
2427	*2105.0	42.9	*438.1	28.4		*2084.0	*1335.0	*3064.0	211.7	*443.9	*1870.0	*1196.0	88.4	*691.5	128.8	*826.7	*1406.0
4271	*2605.0	13.6	647.5		1301.0	*1990.0	*1513.0	*3569.0	256.6	430.8	*2180.0	*1356.0	58.6	*784.9	176.2	*1051.0	*1543.0
5611	*3471.0	55.6	748.4		1461.0	*2717.0	*1843.0	*4951.0	233.2	384.0	*2987.0	*1811.0	52.1	*891.8	155.6	*1222.0	*2018.0
9878	3646.0	53.4	921.8	44.1	*1430.0	*2588.0	*1756.0	*5074.0	208.1	339.8	*2966.0	*1720.0	65.8	*871.3	196.2	1196.0	*2096.0
19566	*3091.0	50.3	387.4	21.8	1239.0	*2202.0	*1477.0	*4288.0	294.1	312.5	*2389.0	*1295.0	27.1	696.3	147.9	*986.0	*1844.0
24656	*3016.0	42.2	255.7	24.2	1055.0	*2074.0	*1337.0	*4118.0	270.6	248.8	2318.0	1148.0	27.8	581.3	134.4	*779.8	*1634.0
29829	*3093.0	52.3	3351.2	81.6	808.9	*1916.0	*1307.0	*4190.0	274.7	261.9	*2328.0	*1106.0	33.0	521.8	120.8	818.5s	*1626.0
32296	*3136.0	33.8	407.8	39.3	938.2	*2020.0	*1271.0	*4333.0	280.0	275.1	*2341.0	*1141.0	37.2	545.9	129.7	813.6	*1540.0

TABLE 2—*Continued*

	N V	Si II	O I	C II	Si IV	O IV]	N IV]	C IV	[Ne V]	[Ne IV]	He II	O III]	N IV	N III]	Si II	Si III]	C III]
RR Tel																	
SWP	*1238.5*	*1265.9*	*1303.2*	*1333.0*	*1393.9*	*1400.8*	*1485.0*	*1547.7*	*1573.0*	*1599.5*	*1639.2*	*1663.4*	*1717.3*	*1749.7*	*1815.8*	*1890.7*	*1907.4*
2047	*27620.	314.8	2134.0	211.6	5273.0	12750.0	6370.0	*42610.	1937.0	1172.0	*19980.	6429.0	216.4	2417.0	438.9	4390.0	*11480.
5885	*14890.	150.8	1800.0	292.6	*5403.0	*8839.0	*5558.0	*18150.	1601.0	1217.0	*9346.0	*5388.0	346.2	2061.0	390.6	*3231.0	*5498.0
8610	23220.0	629.2	1514.0	851.6	4269.0	10690.0	5189.0	*45610.	1899.0	1578.0	*19890.	5155.0		1774.0	295.2	*3011.0	*10510.
28292	*14780.	96.7	650.1		2271.0	6815.0	3167.0	*24670.	1465.0	811.5	*13210.	*3635.0	67.0	1371.0	248.4	2213.0	*6569.0
29536	*15090.		513.1		2221.0	6361.0	3281.0	*24610.	1182.0	713.4	*13680.	3377.0	87.2	1305.0	323.4	2056.0	*6768.0
31080	9518.0		353.5		1726.0	4270.0	1934.0	*20060.	677.0	567.2	10040.0	2058.0	172.7	818.3		1134.0	4508.0
HBV 475																	
SWP	*1239.9*	.....	*1304.6*	*1336.9*	*1395.1*	*1402.1*	*1486.7*	*1549.6*	*1576.1*	*1602.7*	*1640.4*	*1664.1*	*1717.1*	*1751.1*	*1818.5*	*1892.3*	*1909.4*
9900	249.7		79.4	4.8	54.5	109.7	85.8	*902.6	17.3	7.0	520.4	92.1	10.0	50.7	12.5	94.8	189.0
14688	44.8		1.4		12.2	40.3	34.6	229.8	7.5	4.9	172.6	38.2		25.7	0.9	17.8	95.6
16760	52.1				11.8	20.6	31.7	307.1	7.3		193.1	58.8		27.3		25.1	114.1
19575	212.8		56.1		37.3	84.7	68.8	618.5	15.6	7.5	452.3	74.8		38.7	8.0	69.5	137.1
22840	37.0		2.1	4.0		23.5	20.7	168.5	7.7	4.9	164.3	81.0	6.2	28.1	5.3	17.5	77.6
26943	193.3		52.6			75.7	70.8	557.8		2.6	460.9	87.2	3.4	42.4	10.0	62.8	126.2
29815	36.4		4.5		10.1	28.3	17.4	*168.8	1.2		*129.3	22.8	1.8	*22.4	1.2	16.4	*68.1
34313	145.6		32.7	3.6		70.4	50.9	497.0			334.9	51.1		36.6	6.5	40.8	92.7
AG Peg																	
SWP	*1241.3*	.....	*1306.0*	*1332.8*	*1394.2*	*1403.4*	*1486.0*	*1549.5*	*1576.5*	*1600.5*	*1640.0*	*1663.4*	*1719.1*	*1749.8*	*1818.4*	*1890.5*	*1908.4*
2123	*24820.0		1124.0		1042.0	3206.0	*17350.	*32760.	157.5		*23050.	8123.0	7270.0	2422.0		1203.0	2247.0
3795	*3154.0				*358.1	*917.5	*5617.0	*8001.0			*5466.0	*979.9	*2821.0	*795.6	*113.2	*422.5	*837.6
6354	*23940.0		1132.0	696.4	1174.0	2288.0	*12400.	*25710.	290.4		1913.0	5867.0	4709.0	1834.0	260.9	879.2	1592.0
9117	*21930.0		2911.0	746.0	3199.0	5166.0	*14060.	*25690.0			*16810.	*8129.0	3933.0	2497.0	460.4	1837.0	2214.0
10455	*23620.0			409.6	1480.0	2792.0	*1130.0	*22500.0			*16200.	4166.0	3436.0	1512.0	142.3	690.4	1490.0
26023	*16970.0		451.4		2049.0	*5994.0	*7696.0	*16910.0		425.0	*9832.0	*5299.0	924.8	1717.0	408.2	831.4	*1782.0
Z And																	
Active																	
SWP	*1241.3*	*1265.8*	*1305.8*	*1336.1*	*1394.9*	*1403.4*	*1487.7*	*1549.9*	*1577.8*	*1595.9*	*1640.9*	*1665.6*	*1712.1*	*1751.5*	*1817.1*	*1892.0*	*1909.6*
26937	*468.6		68.4	19.0		*343.9	*180.4	*1261.0	77.2		*1477.0	*152.5	26.4	*62.2	16.8	*142.7	*215.8
27028	209.8	40.0	293.5	57.9	598.4	*572.3	320.6	*2182.0			*396.6	876.4		548.2	268.1	*592.0	*698.0
27203	84.7		252.6	32.9	510.9	453.1	195.5	1699.0		134.8	309.2	700.3	58.7	597.6		916.5	1046.0
27632	72.8		272.3		594.7	524.4	206.8	2247.0		101.3	456.4	835.7		409.7	101.1	773.2	842.1
Quiescent																	
	1240.2	*1266.3*	*1305.7*	*1333.1*	*1396.3*	*1402*	*1486.7*	*1549.5*	*1576.6*	*1601.2*	*1640.7*	*1664*	*1720.8*	*1751.3*	*1820.7*	*1891.7*	*1909.5*
5809	388.9		72.1	19.0		343.8	178.6	1260.0	77.4		*1475.0	152.5		62.4	16.7	138.9	215.7
11006	*1341.0	36.6	*383.4		454.4	*694.0	360.2	*1981.0	43.5	18.9	*1417.0	448.4	48.0	160.7	34.8	*365.1	261.5
32208	981.3		94.3		308.0	526.5	245.4	*2193.0	83.1		*1917.0	283.6	41.8	127.5	24.3	141.3	268.1
32845	447.6		34.9		147.5	313.1	180.8	*1491.0	60.5	34.3	*1494.0	195.3	18.5	106.0		106.1	227.4

TABLE 2—*Continued*

	N V	Si II	O I	C II	Si IV	O IV]	N IV]	C IV	[Ne V]	[Ne IV]	He II	O III]	N IV	N III]	Si II	Si III]	C III]
R Aqr																	
SWP	*1242.2*	*1263.6*	*1305.5*	*1335.7*	*1394.1*	*1402.9*	*1489.1*	*1549.1*	*1575.4*	*1600.4*	*1638.4*	*1663.7*	*1722.3*	*1750.8*	*1817.0*	*1892.6*	*1907.9*
3792	54.5	6.3	79.0	52.3	47.3	62.9		250.8	8.7	24.8	48.2	92.2	12.0	115.4	22.5	231.9	*571.0
5856	48.3		56.7	59.9	21.3	78.7		319.5	42.1	36.4	28.3	68.4		68.4		175.0	523.6
16918	30.4		84.3	93.1	62.4	105.6	74.5	*396.9	33.8	22.9	58.6	142.7	13.4	135.0	40.0	267.6	*725.6
20069		235.7	9.6	54.2	33.1	68.6	20.2	298.8			42.5	98.7	16.3	85.9	17.3	160.3	*526.9
26569	27.2	20.2	60.4	69.7	55.7	113.4	15.5	291.0			32.7	114.0	13.5	59.1	12.0	188.7	*510.1
28611	36.1	12.2	125.3	100.5	60.4	91.5	38.3	402.6			42.3	142.4		67.5	14.7	170.3	*521.2
29562	26.4	29.0	107.6	106.1	76.9	112.4	31.6	*428.7	29.0	18.2	47.7	141.4	4.9	83.0	24.1	*250.1	*382.8
32646	35.1	14.0	80.0	104.7	79.0	102.2	15.8	646.4	13.1	8.0	89.5	201.4	18.7	144.5	37.8	293.2	*806.4

NOTES.—Flux units are 10^{-14} ergs cm^{-2} s^{-1} $Å^{-1}$. Measured wavelengths are averages. Laboratory wavelengths are in italics in the header. Measured wavelengths, in italics with each star, are averages. Asterisk (*) indicates a saturated feature.

TABLE 3

GENERAL PROPERTIES OF THE SYMBIOTIC STARS IN THIS ATLAS OBSERVED WITH *IUE*

Star	HD #	Spectal Type[a]	Sym-biotic Type[b]	# of IUE Obs.	E_{B-V}	Radio (6cm) Flux[c] (mJy)	X-ray[§] Flux[d]	Eclip-sing?	Mira Period (days)	Orbital Period (days)	v_r (km/s)	Distance (kpc)	T_{hot} (10^3K)	T_e (10^3K)	n_e (cm^{-3})
EG And	4174	M 2.4 III	S	21	0.05-0.09	<0.26		yes		470-482	-96	0.32-0.63	60-80		
AX Per		M5.2 II-III	S	21	0.25-0.29	<0.71		maybe		682			105	10	$>10^6$
LMC Anon			D	2	0.25-0.30						600			10-20	10^6-10^7
LMC S63		M	S	2	0.02							49-55	50-80	10-20	10^7-10^8
RX Pup	69190	≥M5	D	9	0.3-1.1	≤34			580			1.0-1.3	75-90		
He2-38		≥M5	D	2	0.93				433		113±4	3.8		10-30	10^6-10^7
SY Mus	100336	M4 III	S	9	0.3-0.5			yes		625		1.1	>65		10^{10}
BI Cru		M1 III	D	2	1.5±0.5				280			2.3-3.8	27		
RW Hya	117970	M2 III	S	9	0.01-0.13	<0.26				372		1.3	75-100		10^8-10^9
He2-106		>M5 III	D	2	1.3	≤20			400-450			2.6-9.4			
Hen 1092			S	2											$≥10^8$
T CrB	143454	M4 III	S	12	0.08-0.15	<0.88				227		1.4	30-45		
AG Dra			S	29	0.01-0.06	<0.46	3.6			554			87		10^{10}-10^{11}
HK Sco		K5 III	S	3		<0.36									
CL Sco			S	1	0.1-0.5	<0.42				625		4-8	100		
H1-36 Arae			D	1	0.27	≤46			450-500			7.6			
Y CrA	166813		S	1	0.56	<0.54							150 (?)		
YY Her		M2 II-III	S	3	0.10-0.25	<0.32				150-200		3.6-8.3	50-100		
AS 296		M5 III	S	5	0.43	0.43						2.2			
AS 295B				1		<0.21					66				
AR Pav		M3-4 II-III	S	26	0.1-0.3			yes		605		4.5-5.8			

TABLE 3—*Continued*

Star	HD #	Spectal Type[a]	Symbiotic Type[b]	# of IUE Obs.	E_{B-V}	Radio (6cm) Flux[c] (mJy)	X-ray§ Flux[d]	Eclipsing?	Mira Period (days)	Orbital Period (days)	v_r (km/s)	Distance (kpc)	T_{hot} (10^3K)	T_e (10^3K)	n_e (cm^{-3})
V443 Her		M5 III	S	2	0.2-0.3	<0.44				597	-60	0.9	80		$\sim 10^9$
BF Cyg		M5 III	S	23	0.3-0.4	2.01		maybe		757		1.5-2	40-60		10^9-10^{10}
CH Cyg	182917	M6.5 III	S	23	??	0.4-18	12	maybe		5750	-60		??		10^7-10^9
HM Sge		≥M5 III	D	8	0.40-0.65	15	48		527			1-4 ?	??		?
CI Cyg		M4-5 III	D	40	0.3-0.5	<0.42		yes		855	-20	1.5	150-175	10-14	$\sim 10^{10}$
V1016 Cyg		M4-7 III	D	17	0.2-0.4	45	0.82		472	3467		1.3-6.0	125-160		10^6
RR Tel		≥M5 III	D	13	0.1	28	0.67		374		-53	1.9-2.6	135-150	12-19	10^5-10^7
HBV 475		M4-6 III	S	34	0.3-0.6	1.07		maybe		950-975		1.2-3.4	50&170	15	10^6-10^7
AG Peg	207757	M2-3 III	S	8	0.1-0.2	7.51				733-827		1.3	30-95	11	10^{10}
Z And	221650	M3-6 III	S	44	0.3	1.01				756		1.1	100-150	3.2	$\sim 10^{10}$
R Aqr	222800	M7 III	D	19	0.05-0.10	12	20		386	44 yr.		0.2-0.3	50-150		??

NOTES.—The symbol § indicates X-ray flux at ~0.2 keV in 10^{-12} ergs cm^{-2} s^{-1}, corrected for interstellar extinction.
[a] Kenyon & Fernandez-Castro (1987); Schulte-Ladbeck (1988).
[b] Kenyon (1986).
[c] Seaquist & Taylor (1990); Seaquist (1988).
[d] Viotti (1993).

1994ApJS...94..183M

TABLE 4

QUALITATIVE SPECTRAL FEATURES OF THE SYMBIOTIC STARS IN THIS ATLAS

Star	Fig. #	Principal Resonance Lines (N V, C IV, He II)†	Principal Intersystem Lines (O IV, N IV, O III, N III, Si III, C III)] ‡	Continuum Flux	Continuum Shape	Comments
EG And	1	C IV dominates except at $\Phi=0.2$, 0.8	variable with phase	absent at min.	↗ blue	vanishing continuum at $\Phi=0.0$ implies eclipse
AX Per	2	2-3x stronger at optical maximum	weaker at optical minimum	strong at max.	flat, ↗ red	C III] and O III] ↘ with time
LMC Anon	3	N V stronger than He II, C IV	N IV], N III] very strong	weak	flat, ↗ blue	possible CNO processing
LMC S63	4	C IV strong	C III] strong		↗ blue steeply	hot star and an M III
RX Pup	5	C IV, He II strong	C III] strong		flat, ↗ red	intersystem emission decreasing since 1980-82
He2-38	6	C IV strong	O III], C III] strong	noisy		spectra weak
SY Mus	7	2x less at $\Phi=0.0$; C IV, He II strong	weak in UV	drops at min.		N V and C IV very prominent out of eclipse
BI Cru	8	N V present	O III], Si III] strong	noisy		noisy even when co-added
RW Hya	9	many broad, high ionization lines seen	forbidden doubly ionized lines weak	low on one obs.	↗ blue	possibly eclipsing, in compact high density nebula
He2-106	10	C IV, He II seen	O III], C III] seen	> 1600 Å, weak		noisy, even when co-added
Hen 1092	11	C IV, He II equally strong	very weak > 1700 Å		flat	very dense nebula ?
T CrB	12	strong when continuum strong	strong when continuum strong	varies	flat	substantial variation in continuum and line flux
AG Dra	13	He II stronger than C IV in both states	weak in both outburst & quiescent states	very strong at outburst	↗ blue at outburst	15 year activity cycle for outbursts - anomalous outburst in 1985, 86
HK Sco	14	N V, C IV, He II observed	weak in UV	noisy	flat	1982 C IV, He II > 1981 C IV, He II
CL Sco	15	C IV predominates	O III], Si III], C III] unusually strong	noisy	↗ red	low density, photoionization region ?
H1-36 Arae	16	C IV, He II broad	N III], C III] broad	none		broad emission lines
Y CrA	17	strong, narrow He II	narrow	weak	flat	main sequence, accreting star ?
YY Her	18	all strong	O IV], N IV], O III] strong; weak > 1700 Å	constant	flat	much weaker in 12/81 and in 5/80
AS 296	19	↘ after outburst	↗ after outburst, especially > 1600 Å	noisy, weak	~ flat	outburst in 1988 June
AS 295B	20	C IV, He II broad	broad	none		only one IUE spectrum available

TABLE 4—*Continued*

Star	Fig. #	Principal Resonance Lines	Principal Intersystem Lines	Continuum Flux	Continuum Shape	Comments
AR Pav	21	stronger by 2x out of eclipse	weaker during eclipse	weak in eclipse	↗ red non-eclipse	effects of eclipse are very noticeable
V443 Her	22	N V, C IV strong	O IV], N III], Si III], C III] strong	strong	flat	11/80 spectrum ~1.25x strength of 5/80
BF Cyg	23	N V, O I very weak, except at visual maximum	prominent; weaker during eclipse	very strong	↗ blue at max. flat at min.	possibly eclipsing; emission in '86-'88 > '79-'80
CH Cyg	24	strength varies with system state	strength varies with state of the system	varies erratically	often flat; ↗ red	several active phases; opaque, circumstellar, iron shell
HM Sge	25	all lines intense	many intense lines	almost none	flat	variable emission intensity
CI Cyg	26	stronger during '82 eclipse than '80	brighter during '80 eclipse than '82	weak; 0 at min.	flat	excitations vary from one eclipse to another
V1016 Cyg	27	very strong; 2x at UV maximum	very strong, 1.5x at UV maximum	weak	flat	[Ne IV], [Ne V] present
RR Tel	28	strong, ↘ from '78 to '87	strong, gradually decreasing	very weak	flat	consistent with a slow nova on the decline
HBV 475	29	C IV, He II, strongest at visual max.	somewhat weak, vary with visual phase	very weak	flat	consistent with an eclipsing binary
AG Peg	30	strong	N IV] exceptionally strong, weaker > 1700 Å	strong	↗ blue	one of the brightest; has a dense nebular region
Z And	31	strong, He II much stronger in quiesence	strong, 2-3x as much during outburst	outburst: strong quies.: moderate	↗ red flat	relative strength of intersystem lines greater at outburst, implying material from cool component being photoionized
R Aqr	32	N V weak, C IV dominates	C III] dominates, most are present	strong	flat	has a jet seen in both radio and UV

NOTES.—Dagger (†) indicates N V λλ 1238,1240; C IV λλ 1548; 1550; He II λ1640. Double dagger (‡) indicates O IV] λλ 1397, 1407; N IV] λ1487; O III] λλ 1660, 1666; N III] λλ 1747, 1753; Si III] λ1892; C III] λλ 1906, 1909. The arrow pointing up (↗) means "increasing toward," and the arrow pointing down (↘) means "decreasing toward."

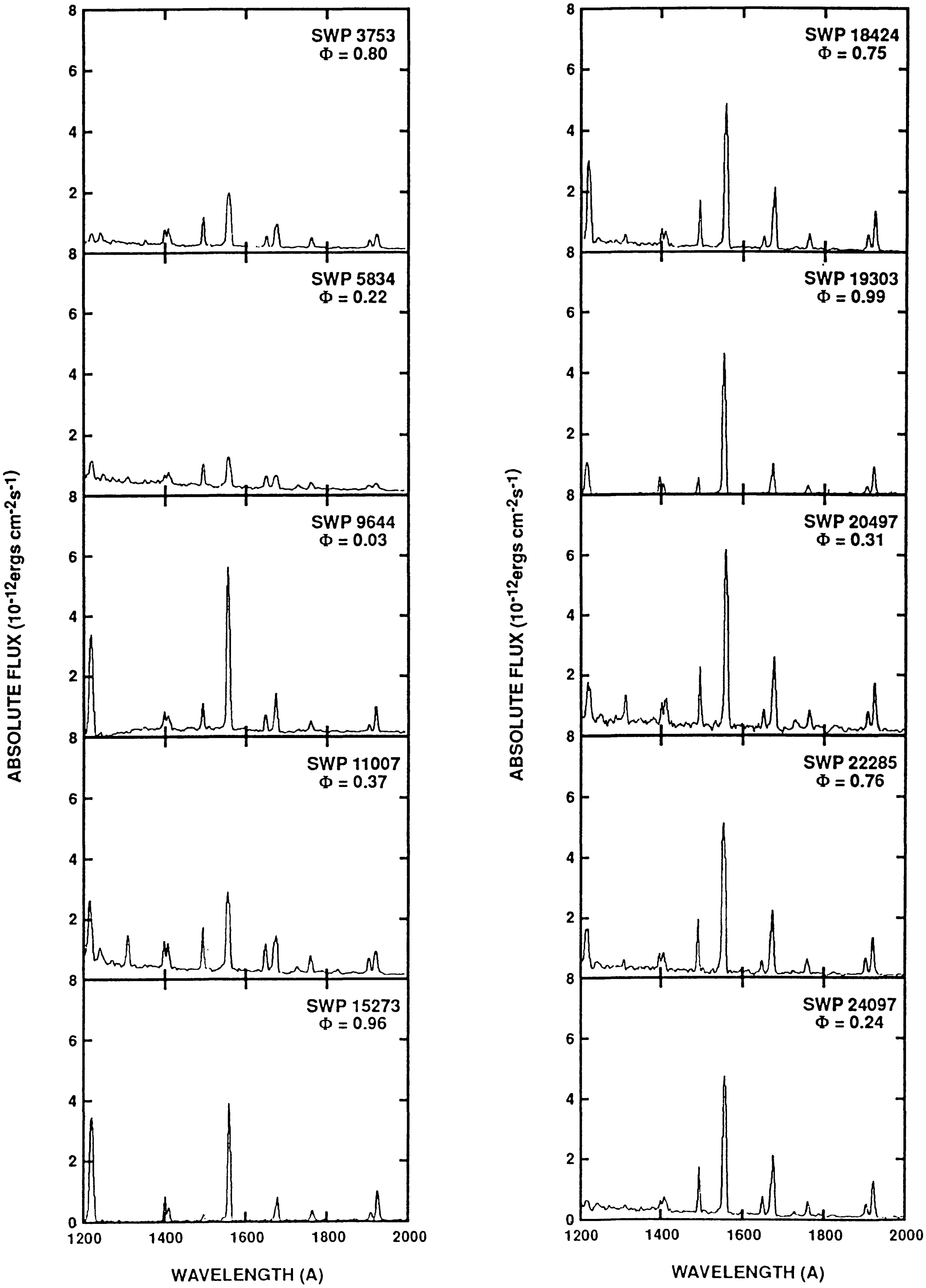

FIG. 1.—Low-resolution *IUE* spectra of EG Andromedae obtained in the SWP λλ 1200–2000 wavelength region. The spectra were taken at orbital phases determined by Chochol et al. (1987) with min (*UBV*) = JD 2,446,336.7 + 474.0^d*E*.

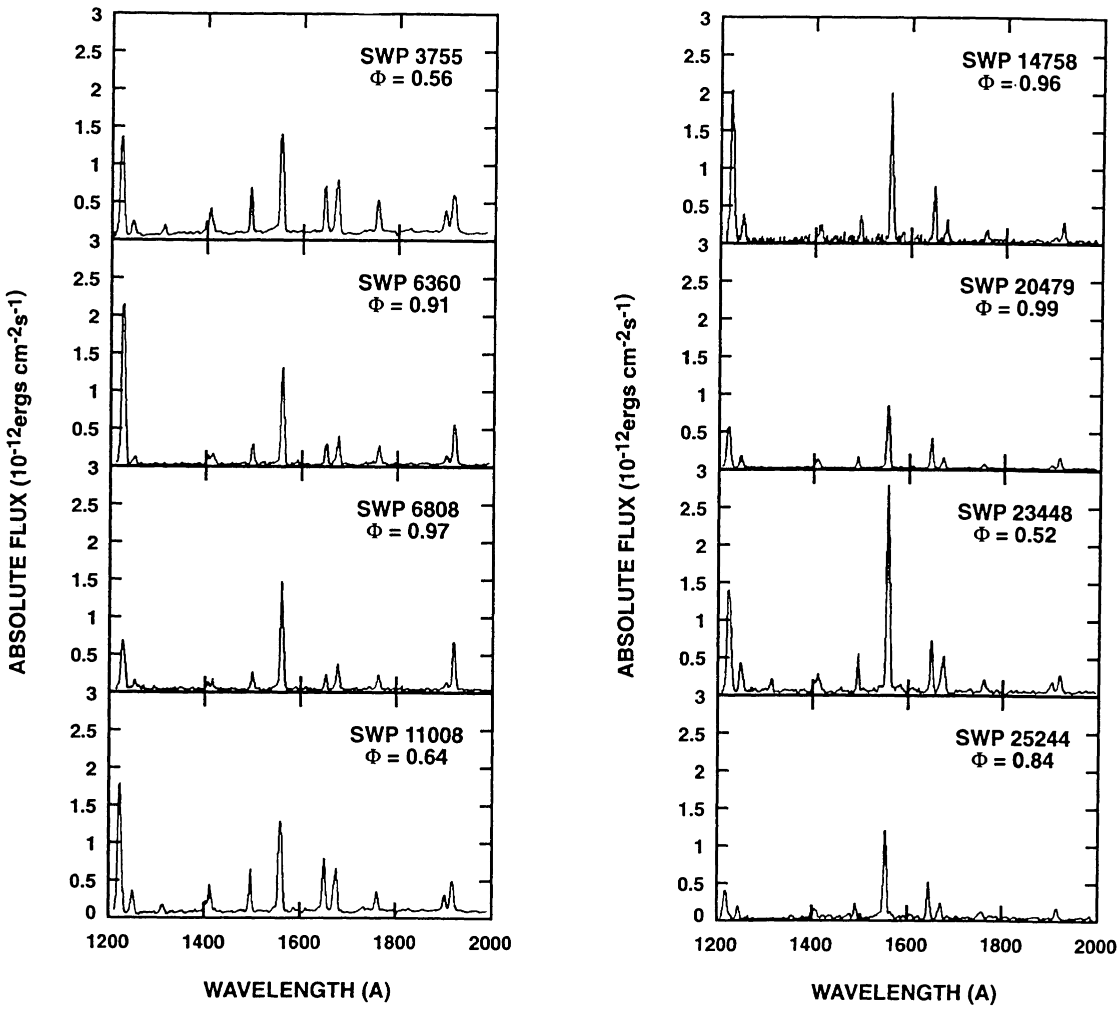

FIG. 2.—Low-resolution SWP spectra of the symbiotic star AX Persei. Orbital phases were found from an ephemeris by Kenyon (1982) using min (pg) = 2,436,679.4 + 681.6^{d}E. The UV continuum increases toward longer wavelength when the star is near a maximum.

near maximum, showing a slight rise toward longer wavelengths. UV emission line intensities vary by factors of 2–3 from optical minimum to maximum. C IV λλ 1548,1550 is the most prominent emission line in the spectra. The strength of the O III] λλ 1660,1666 and C III] λλ 1907,1909 emission lines seen (Fig. 2) steadily decrease, while the He II λ1640 emission line increases, consistent with progressively higher density regions coming into view during this orbital phase. The UV flux distribution of AX Per is similar to that of CI Cyg because they are both relatively flat (independent of wavelength) and exhibit intense narrow emission lines (Kenyon 1986).

4.3. LMC Anon

Three UV spectra of LMC Anon have been co-added (Fig. 3) to increase the signal-to-noise ratio. The UV continuum is very weak but shows a slight increase toward shorter wavelengths consistent with hot, stellar blackbody emission. N V λλ 1238,1242, N IV] λ1487 and N III] λλ 1747–1753 are the strongest emission lines present in the spectrum (Table 3). High ionization lines of C IV and He II, which are present in most symbiotics, are not nearly as intense compared with N V and

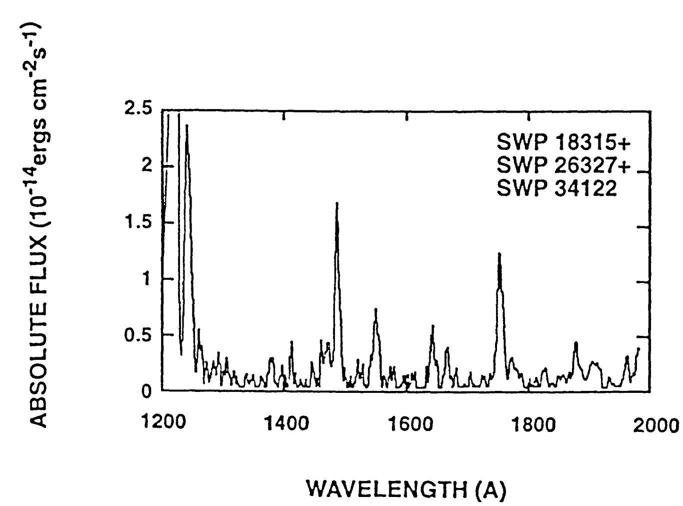

FIG. 3.—Three co-added spectra of LMC Anon are shown. These spectra are not well exposed. N V λλ 1238,1240, N IV] λ1487, and N III] λλ 1747–1753 are particularly strong.

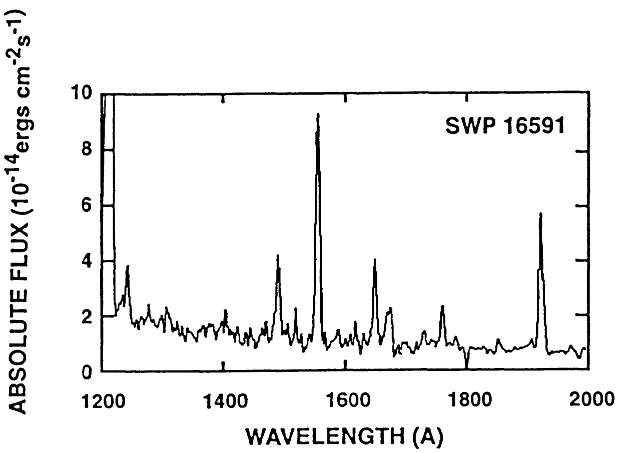

FIG. 4.—This spectrum of LMC S63, obtained in 1982 March, exhibits a UV continuum increasing toward shorter wavelengths, characteristic of a hot star with $T_{\rm eff} > 25{,}000$ K.

N IV], which are about 2–3 times stronger than the He II and C IV lines, respectively. The presence of relatively weak carbon and strong nitrogen emission lines suggests evidence of CNO processing (Kafatos et al. 1983).

4.4. *LMC S63*

The UV spectrum of LMC S63 shown in Figure 4 exhibits a continuum flux distribution which increases steeply toward shorter wavelengths and contains many allowed and semiforbidden emission lines (e.g., N V, N IV], C IV, He II, O III], N III], and C III]), with C IV and C III] being the strongest. The slope of the UV continuum and the various emission lines present in the spectrum of LMC S63 indicate the presence of a hot stellar component and a cool M giant one.

4.5. *RX Puppis*

RX Pup is a D-type symbiotic star similar to a slow nova (Swings & Allen 1972). Six of the nine ultraviolet observations of RX Pup taken between 1980–1986 are in Figure 5. The far-UV spectrum of RX Pup exhibits a variety of strong emission lines that are superposed on a continuum, which sometimes increases toward longer wavelengths. C IV and C III] are the most prominent emission lines present in the UV spectrum of RX Pup. The intersystem emission lines of O III], N III], Si III], and C III] decreased in intensity during the period 1980 to 1986.

4.6. *He 2-38*

The two spectra of He 2-38 shown in Figure 6 have been co-added to increase the signal-to-noise ratio. Only the strongest emission lines were detected above background. The strongest lines in the SWP range are N V λλ 1238,1242, C IV λλ 1548,1550, He II λ1640, O III] λλ 1660,1666 and C III] λλ 1907,1909.

4.7. *SY Muscae*

SY Mus exhibits dramatic UV variability which depends on the phase of the 625 day orbital period. The ephemeris of Ken-

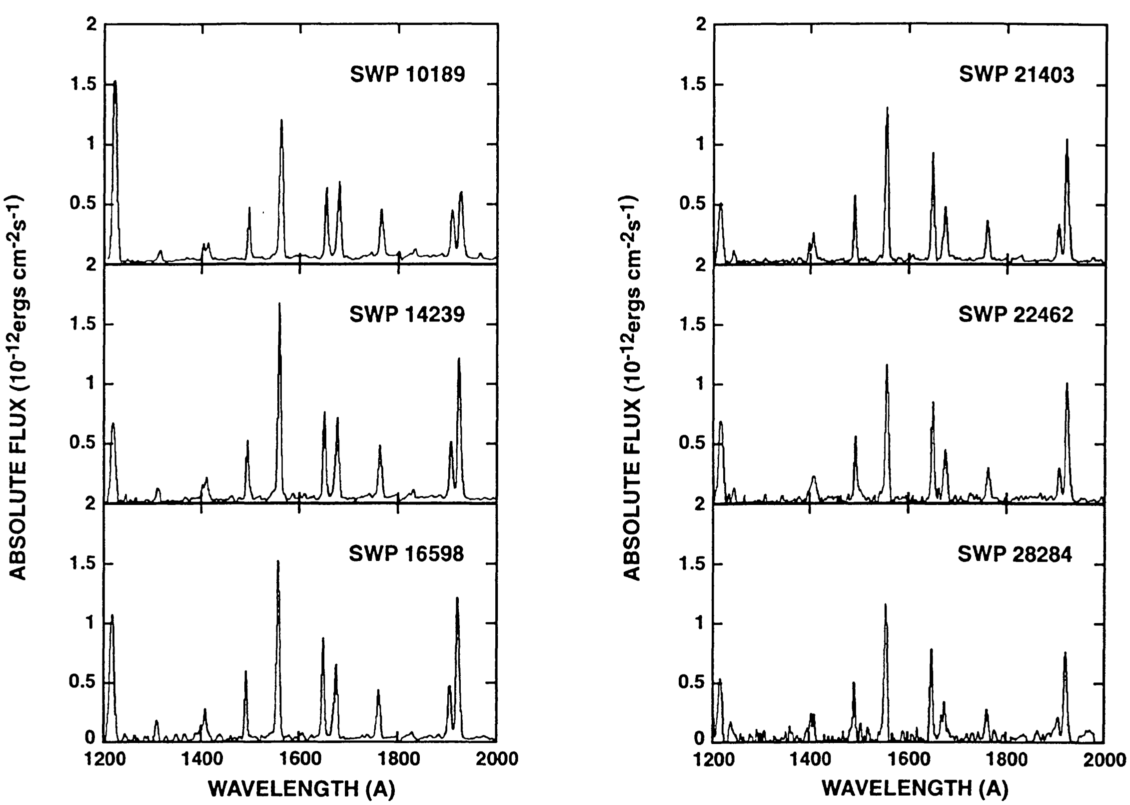

FIG. 5.—Low-resolution *IUE* spectra of RX Puppis, covering 1980 September to 1986 May

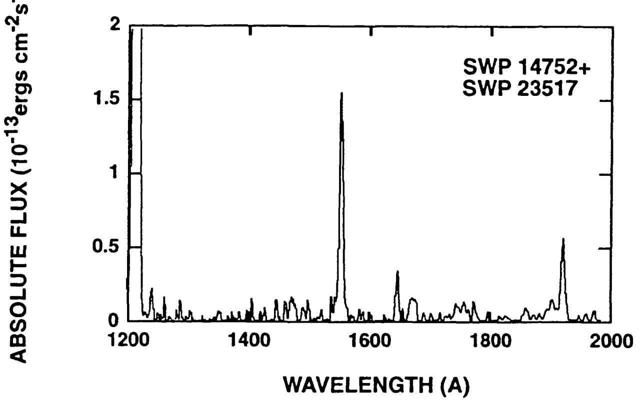

FIG. 6.—Two low-resolution SWP spectra of He 2-38 have been co-added to increase the signal-to-noise ratio. The UV continuum is very weak.

yon & Bateson (1984) was used to determine the phase for each spectrum in Figure 7. At minimum ($\Phi = 0.0$), the continuum drops noticeably, and the emission line strengths decrease by factors of 3–4. N V, C IV, and He II are very prominent out of eclipse at $\Phi \sim 0.5$ (± 0.1), indicating the presence of the hot star. C IV λλ 1548,1550 and He II λ1640 are the most intense lines in all the *IUE* spectra of SY Mus. The intersystem lines of O III], N III], Si III], C III] are generally weak, suggesting high densities $n_e \geq 10^8$ cm^{-3} (Michalitsianos et al. 1982).

4.8. *BI Crucis*

Two SWP spectra of BI Crucis (Fig. 8) were co-added for noise reduction. Even so, the UV spectrum of this symbiotic is characterized by a noisy continuum, if any, with a UV flux distribution which increases toward shorter wavelengths. Only a few emission lines can be clearly identified in the enhanced spectrum.

4.9. *RW Hya*

The SWP spectra of RW Hya in Figure 9, obtained between 1979 and 1987, exhibit a UV continuum flux distribution which increases noticeably toward shorter wavelengths, consistent with hot stellar blackbody emission. The presence, in some cases, of many broad, high-ionization emission lines (e.g., Si IV + O IV] λλ 1393–1407, N IV] λ1487, C IV λλ 1548,1550, He II λ1640, and O III] λλ 1660,1666) suggests a hot photoionized nebular region. The emission-line intensities are 2–3 times smaller in SWP 31038 than those found in the

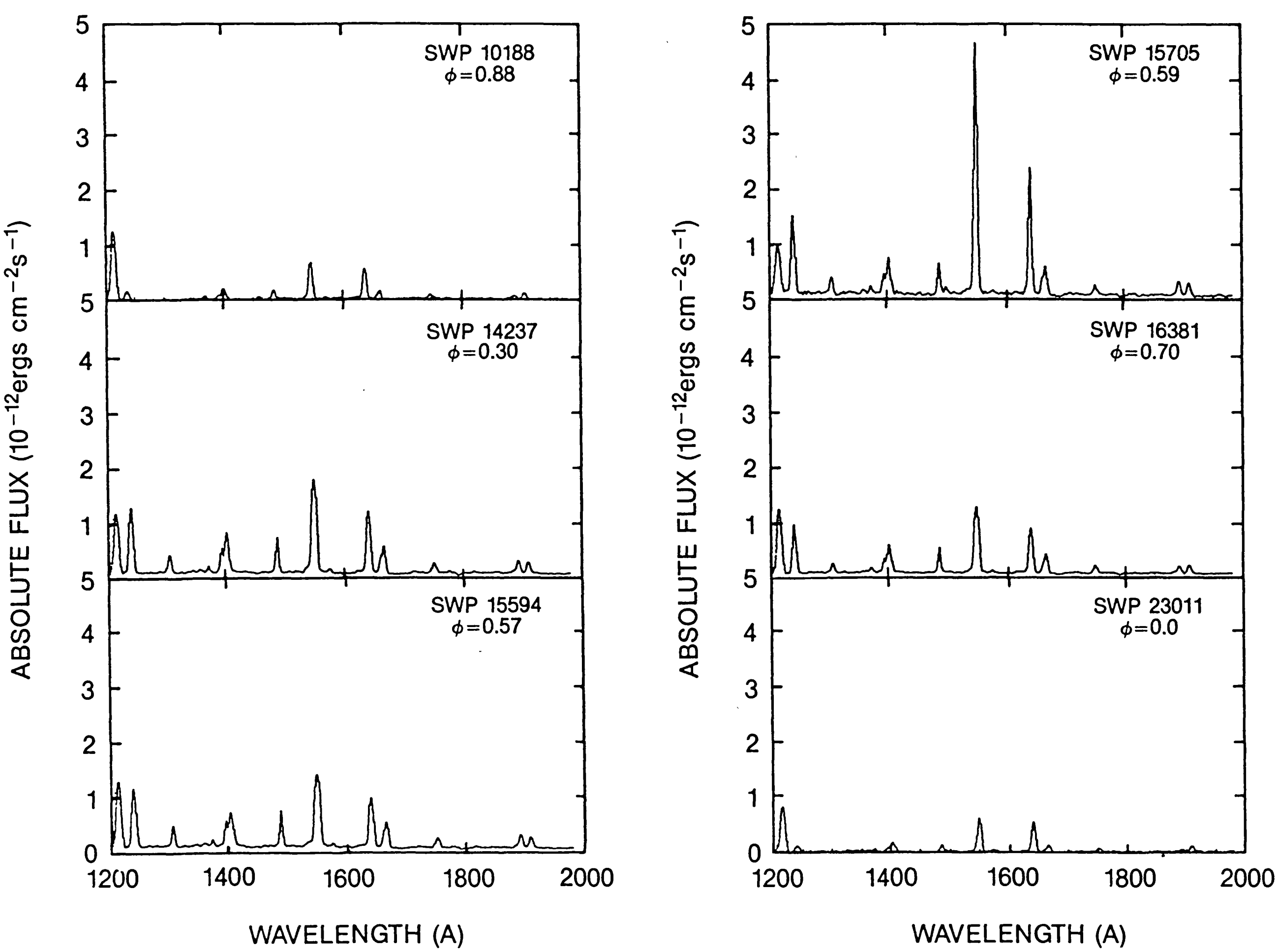

FIG. 7.—Low-resolution *IUE* far-UV spectra of the symbiotic star SY Muscae. These spectra exhibit a nearly flat UV continuum near visual minimum ($\Phi = 0.0 \pm 0.1$). All orbital phases were determined from the ephemeris min (V) = JD 2,435,175.7 + 627.0$^d E$ (Kenyon & Bateson 1984).

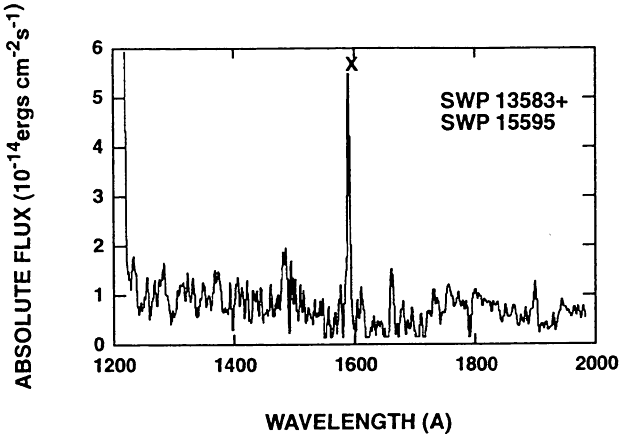

FIG. 8.—The low-resolution *IUE* spectrum of BI Crucis. Two spectra of BI Cru have been co-added to increase the signal-to-noise ratio. Even so, the UV continuum is still noisy. X indicates a cosmic-ray hit.

preceding 1985 June (SWP 26220) spectrum. The lack of continuum and the significant decline in emission-line strength suggests that RW Hya is possibly an eclipsing system. The weakness of forbidden lines N III] λλ 1747–1753, Si III] λ1892, and C III] λλ 1907,1909 implies that the compact nebula in which both the primary and secondary stars are embedded has particularly high densities, in agreement with Kafatos, Michalitsianos, & Hobbs (1980). Further observations should be made to determine if RW Hya is an eclipsing system.

4.10. *He 2-106*

The UV spectrum of He 2-106 (Fig. 10) is generally noisy, but UV continuum emission is present longward of 1600 Å. C IV λλ 1548,1550, He II λ1640, O III] λλ 1660,1666 and C III] λλ 1907,1909 are the most prominent emission lines in the SWP range. Gutierrez-Moreno, Moreno, & Cortes (1986) suggest that He 2-106 is an optically thick D-type object that exhibits an IR excess due to circumstellar dust.

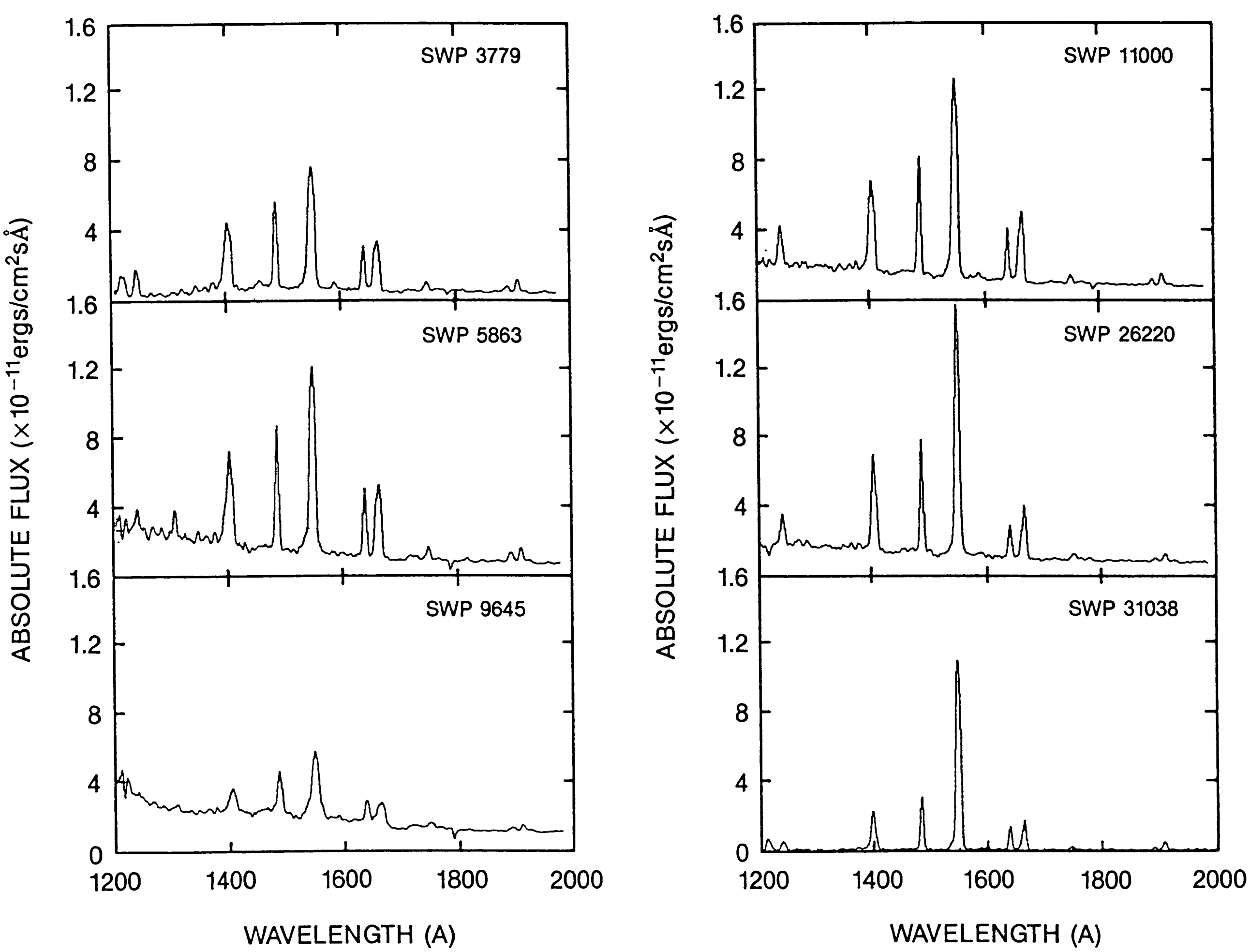

FIG. 9.—Low-resolution SWP spectra of RW Hydrae obtained between 1979 January and 1987 May. The majority of spectra have a far-UV continuum which increases toward shorter wavelengths, consistent with a hot subdwarf.

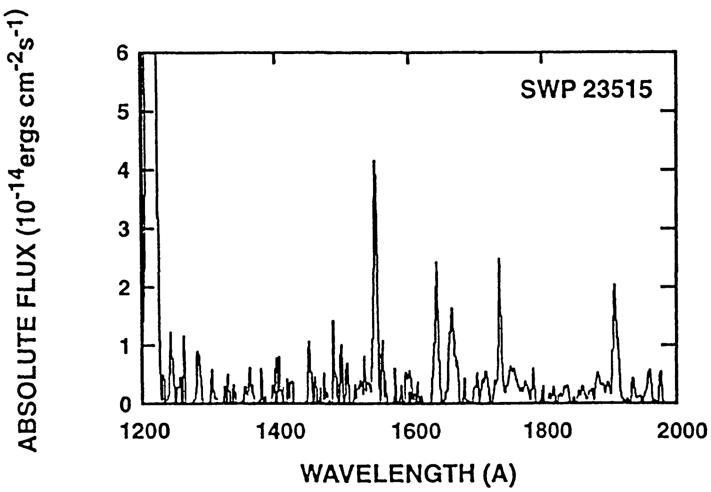

FIG. 10.—An SWP low-resolution spectrum of the symbiotic star He 2-106 taken in 1986 July. The UV continuum is underexposed and noisy, with a few narrow emission lines of C IV, He II, and C III]. X denotes a cosmic ray hit.

4.11. *Hen 1092*

The *IUE* spectrum of Hen 1092 (Fig. 11), taken in 1980 March, has a relatively flat continuum flux distribution with both permitted and intersystem emission lines of N V, O IV], N IV], C IV, He II, O III]. He II λ1640 having comparable intensity to C IV λλ 1548,1550 suggests that the high-excitation permitted line forming region is quite hot, probably in the range 65,000 ≤ T_{hot} ≤ 100,000 K. The weak semiforbidden lines beyond 1700 Å of N III] λλ 1747–1753, Si III] λ1892, and C III] λλ 1907,1909 could indicate a very dense nebula where $n_e \geq 10^8$ cm^{-3}.

4.12. *T Coronae Borealis*

Figure 12 displays the variable UV continuum of T CrB at several stages. Emission lines are more pronounced when the UV continuum flux is strong and become weak when the continuum decreases. With increasing UV continuum flux, N V, C IV, He II, O III], Si III], and C III] become more prominent, the brightest line being C IV λλ 1548,1550. Spectra taken in 1979 (SWP 3815 and SWP 5804) exhibit vastly different continuum levels compared with more recent spectra. The two spectra taken in 1986 (SWP 27556 and SWP 28715) suggest large variations in the continuum level. These continuum variations with timescales of about 1 yr could be associated with accretion. Kenyon & Garcia (1986) suggest that an accreting main-sequence star, rather than a white dwarf, that gains $\sim 10^{-6}$ $M_\odot$ yr^{-1} is the hot companion. Fluctuations associated with an optically thin disk may be responsible for the substantial variations in the UV continuum and emission-line flux observed.

4.13. *AG Draconis*

The *IUE* spectra taken of AG Dra are characterized by either a strong continuum rising toward shorter wavelengths in outburst or a flat, weak continuum in quiescence. Both phases are associated with intense permitted emission lines (e.g., N V, C IV, He II), and weak intersystem emission lines (e.g., N III], Si III], C III]) (Fig. 13). Emission-line intensities increase by a factor of 3 to 6 during active phases, compared with quiescence. The continuum level was considerably higher in the 1980/1981 outburst (SWP 11002, SWP 15709) than in the 1985/1986 outburst (SWP 27542). N V, C IV, and He II are the strongest emission lines in both active and quiescent states, while Si III] and C III] are always weak or absent, consistent with a high-density nebula ($10^{10} \leq n_e \leq 10^{11}$ cm^{-3}) (Kafatos, Meier, & Martin 1993).

4.14. *HK Scorpii*

One of the least studied symbiotics, HK Sco exhibits a relatively weak UV continuum that is relatively flat and noisy. However, N V λλ 1238,1242, C IV λλ 1548,1550 and He II λ1640 are both present suggesting a hot source 65,000 ≤ T_{hot} ≤

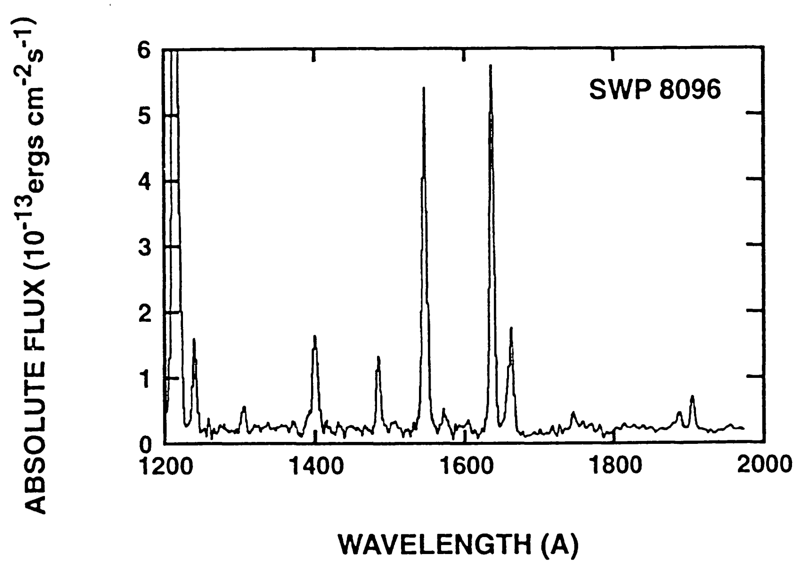

FIG. 11.—The far-UV spectrum of Hen 1092 obtained in 1980 March. This star has a flat continuum and strong emission lines of C IV λλ 1548,1550 and He II λ1640.

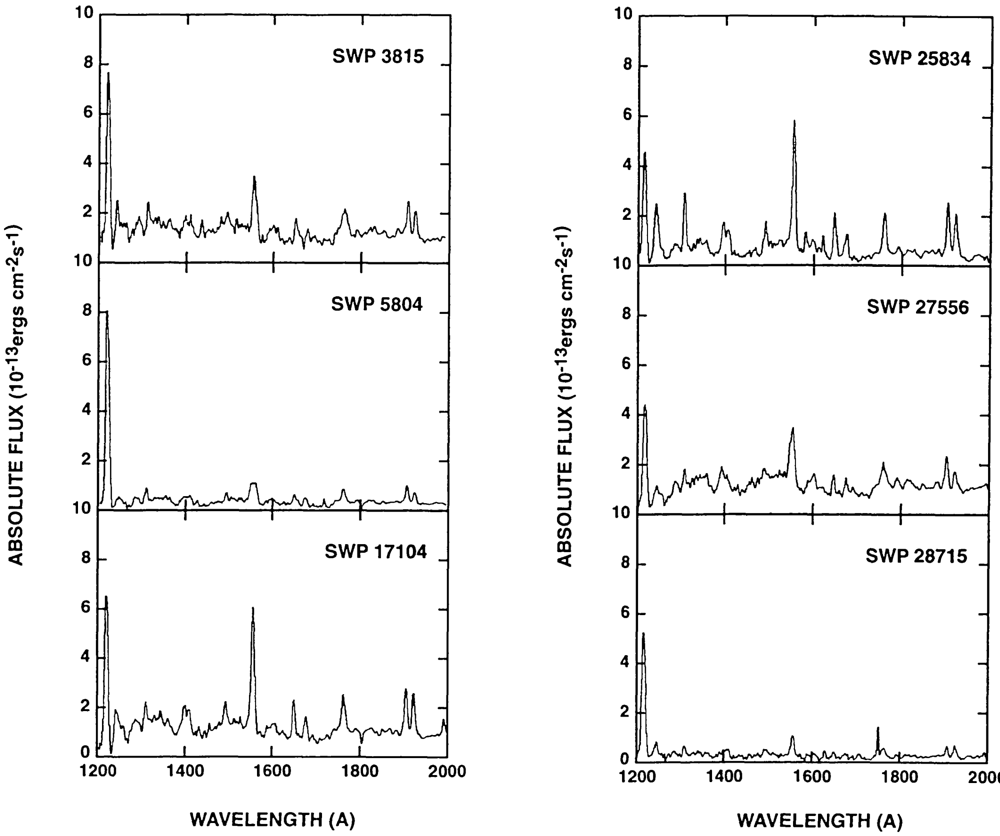

FIG. 12.—*IUE* low-resolution spectra of T Coronae Borealis. Most of the UV spectra shown exhibit a strong and variable continuum with many broad emission lines.

100,000 K in the line-forming region; the conspicuous weakness of semiforbidden lines also suggests the densities are $n_e \leq 10^{10}$ cm^{-3}. A decrease in continuum and emission line intensity is evident in the spectra shown in Fig. 14 obtained in 1981 March and 1982 February. Between these two observations the C IV flux decreased by a factor of 4 and He II by a factor of 2.

4.15. *CL Scorpii*

Although the spectrum of CL Sco (Fig. 15) is rather noisy, the continuum rise with increasing wavelength is evident. The semiforbidden lines of O III], Si III], C III], as well as C IV are the strongest emission lines in the spectrum, while N V, C II, O IV], N IV] and others shortward of 1500 Å are weak. The strong intersystem lines are evidence of a low-density photoionized region, i.e., $10^4 \leq n_e \leq 10^8$ cm^{-3}.

4.16. *H1-36 Arae*

In this UV spectrum of H1-36 Arae (Fig. 16), the most prominent lines are the broad emission profiles of C IV λλ 1548,1550, He II λ1640, N III] λλ 1747–1753 and C III] λλ 1907,1909. The continuum is underexposed.

4.17. *Y CrA*

The far-UV spectrum of Y CrA in SWP 6820 (Fig. 17) is relatively weak. This early *IUE* exposure shows a low, flat continuum and several allowed and intercombination lines of N V, O IV], N IV], C IV], He II, O III], N III], Si III], and C III].

4.18. *YY Herculis*

The far-UV spectrum of YY Her is dominated by the emission lines of N V, N IV], C IV, He II, and O III] superimposed on a flat continuum (Fig. 18). Many semiforbidden lines (i.e. N III], Si III], and C III]) in the spectrum longward of 1700 Å are very weak. The emission line intensities decreased generally by a factor of 2 to 3 between 1980 May and 1981 December. Over this 1.5 yr period, the intensity in N V and O I decreased by factors of 6 and 4, respectively, consistent with YY Her being an eclipsing system. However, the continuum flux did not decrease together with the emission line fluxes, except below 1400 Å, suggesting the regions in which free-free and free-bound emission originate are more extended than the line forming regions.

4.19. *AS 296*

The *IUE* spectra of AS 296 are noisy and exhibit a weak continuum. In the spectra shown here, C IV λλ 1548,1550 is the only prominent high-excitation line. The first two spectra in Figure 19 were taken in 1982 February (SWP 16380) and 1982 November (SWP 18389). Six years later, spectra were obtained 3 months prior to the 1988 March outburst (SWP 33047) and 5 months following that outburst (SWP 34725)

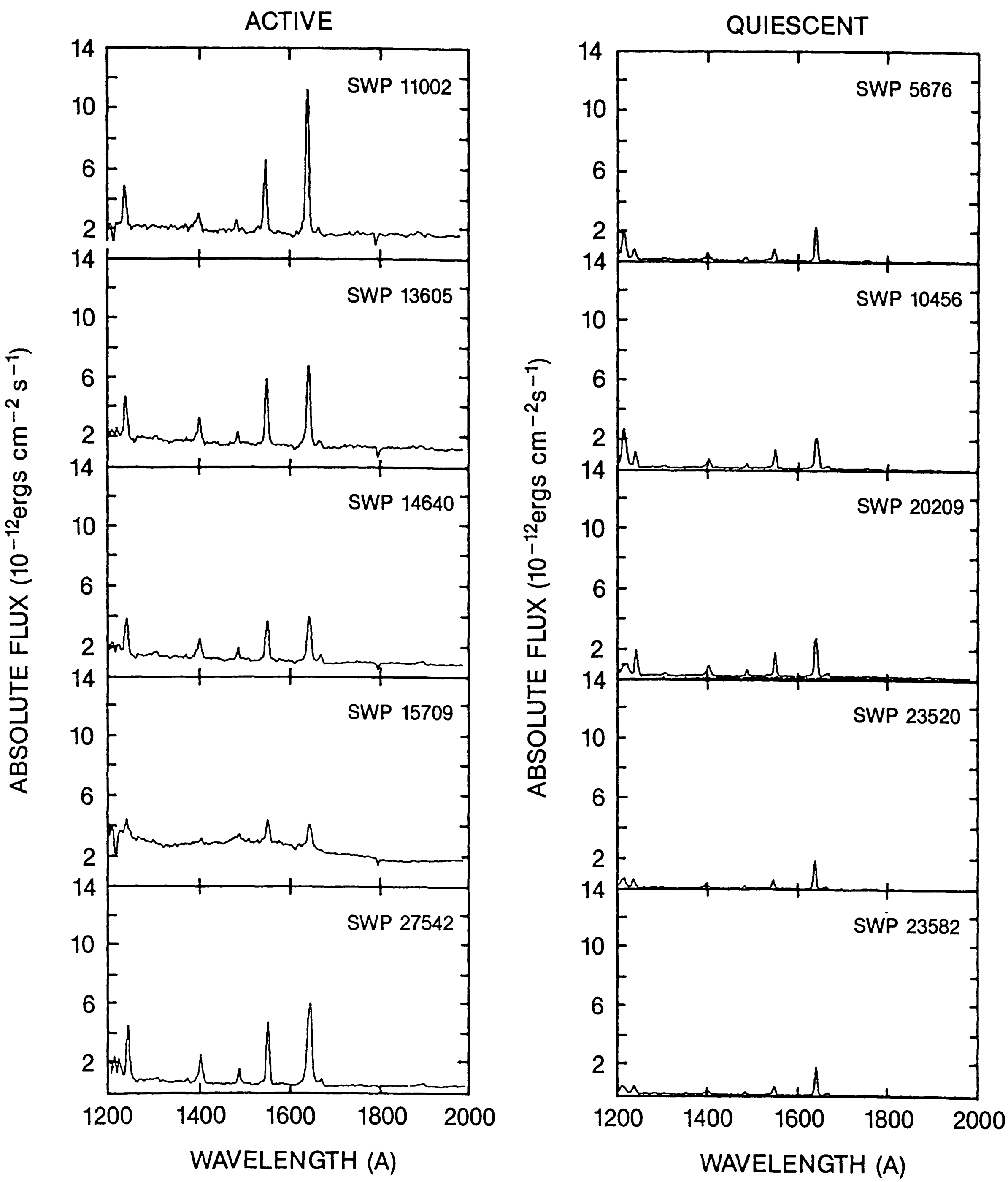

FIG. 13.—Low-resolution SWP spectra of AG Draconis. These spectra are representative of the system in active and quiescent states. Note the variations in the UV continuum between activity and quiescence.

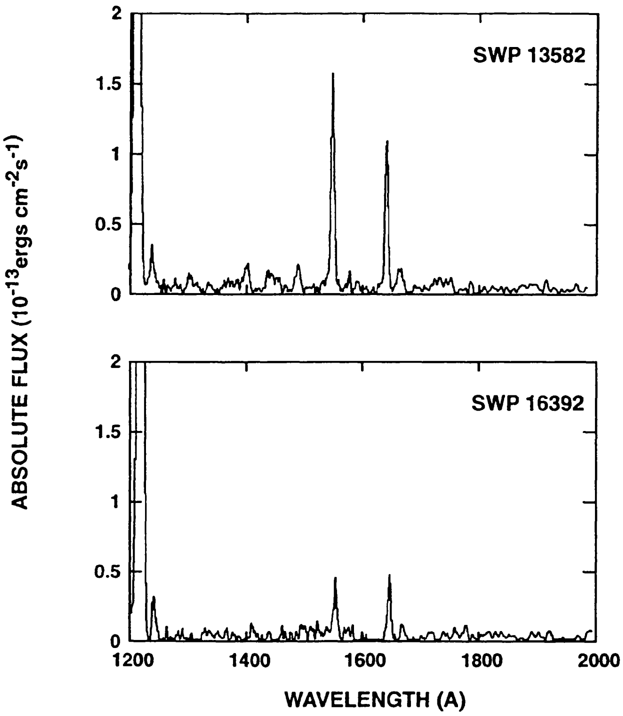

FIG. 14.—Low-resolution *IUE* spectra of the symbiotic star HK Scorpii. The spectra exhibit strong emission lines of C IV and He II superposed on a weak UV continuum.

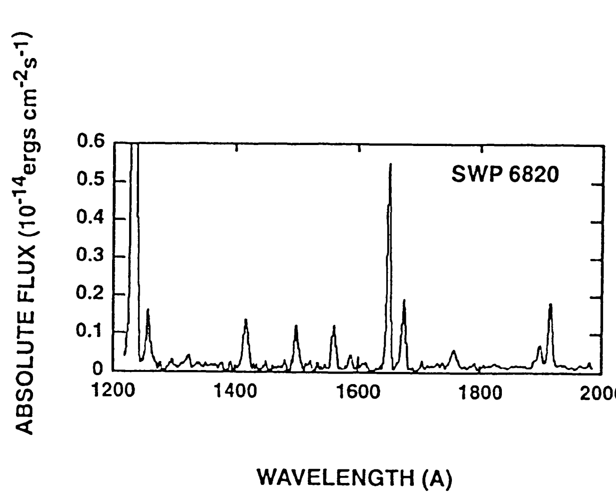

FIG. 17.—Low-resolution spectrum of Y CrA obtained in 1979 October. Y CrA exhibits weak emission lines that are superposed on a flat UV continuum.

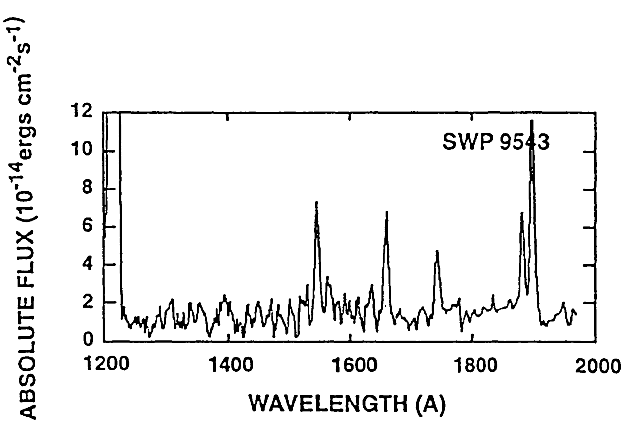

FIG. 15.—A low-resolution SWP spectrum of CL Scorpii taken in 1980 July. Weak UV continuum appears to rise with increasing wavelength.

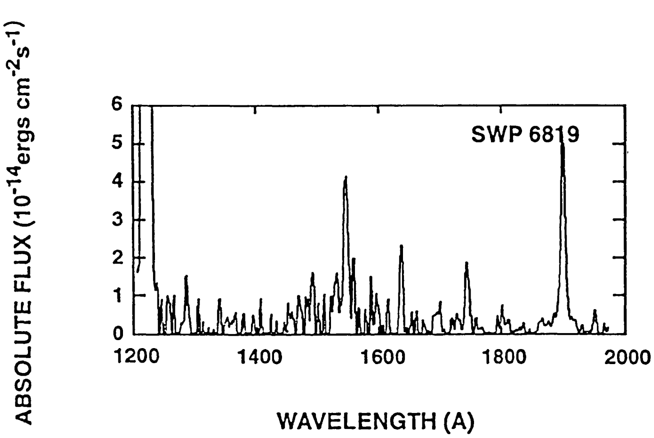

FIG. 16.—This low-resolution SWP spectrum of H1-36 Arae was obtained in 1979 October. The spectrum is not well exposed, but broad emission lines of C IV and C III] are detected.

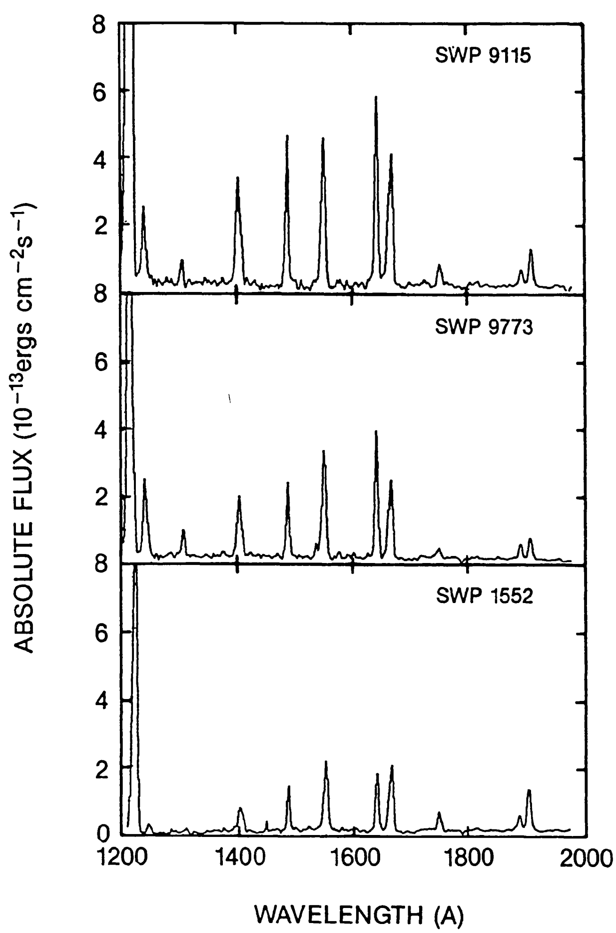

FIG. 18.—Low-resolution *IUE* spectra of YY Herculis. The spectra show permitted and intersystem emission lines on a relatively flat UV continuum flux distribution.

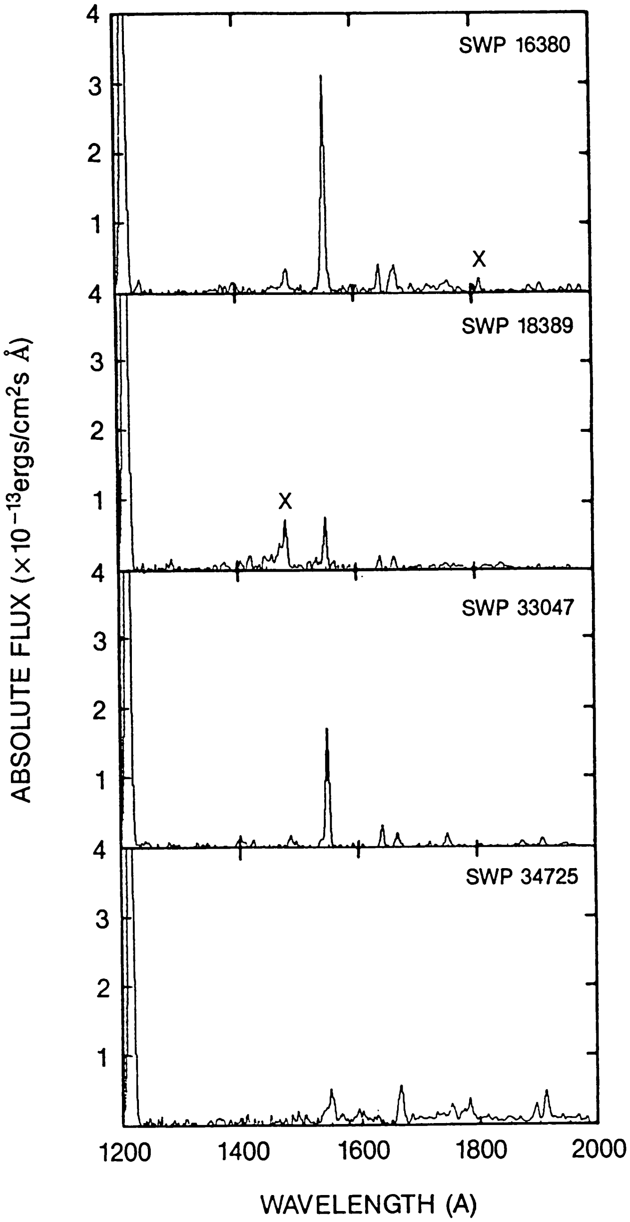

FIG. 19.—Low-resolution SWP spectra of the symbiotic star AS 296. All spectra are underexposed. C IV λλ 1548,1550 is the most prominent emission line. X indicates a cosmic ray hit.

(Munari 1988). The latter of these suggests an increase in the continuum flux longward of 1600 Å and an increase in the intensity of many of the intersystem lines (e.g., O III], Si III], and C III]). This increase in the intersystem line strength, coupled with a decrease in the principal permitted lines of C IV and He II could indicate that the atmosphere of the M giant has been photoionized by the hot star.

4.20. *AS 295B*

The UV spectrum of AS 295B in Figure 20 shows broad emission lines of C IV λλ 1548,1550 and He II λ1640. As with H1-36 Arae, underexposure has left no trace of a continuum.

4.21. *AR Pavonis*

IUE ultraviolet spectra of AR Pav in and out of eclipse (Fig. 21), indicate that the UV continuum and emission lines strongly depend on the orbit phase. When AR Pav is out of eclipse (SWP 5829, SWP 13956) (Andrews 1974) the continuum flux rises noticeably with increasing wavelength and the emission lines tend to be stronger; C IV λλ 1548,1550 and He II λ1640 fluxes also increase by a factor of 2. During a minimum visual phase there is an overall decrease in continuum and emission line intensities expected because the hot star is partly occulted. This decrease can be seen in SWP 10510, SWP 16857, and SWP 17070, which show the presence of continuum and emission lines around phase $\Phi = 0.0$ (± 0.1).

4.22. *V443 Herculis*

The far-UV spectra of V443 Her shown in Figure 22 indicate a relatively strong and flat continuum with many intense emission lines superposed. Both spectra show strong Si IV, O IV], N IV], C IV, He II, and O III] emission. The emission-line intensities increased by about 15% during the 6 month period from 1980 May (SWP 9122) to 1980 November (SWP 10439).

4.23. *BF Cygni*

The UV spectra of BF Cyg (Fig. 23) indicate a strong UV continuum which increases toward shorter wavelengths, except near visual minimum, $\Phi = 0.0$, when the hot star is in eclipse. The UV continuum flux distribution varies with the photometric ephemeris determined by Mikolajewska (1987), consistent with an occultation of the hot companion star. The spectra at minimum show a flat continuum with weak N V and O I (SWP 13477 and SWP 30924), while spectra near maximum exhibit a strong UV continuum and emission lines. Many of the intersystem lines are particularly prominent, such as O III], N III], Si III], and C III]. The N V and O I permitted

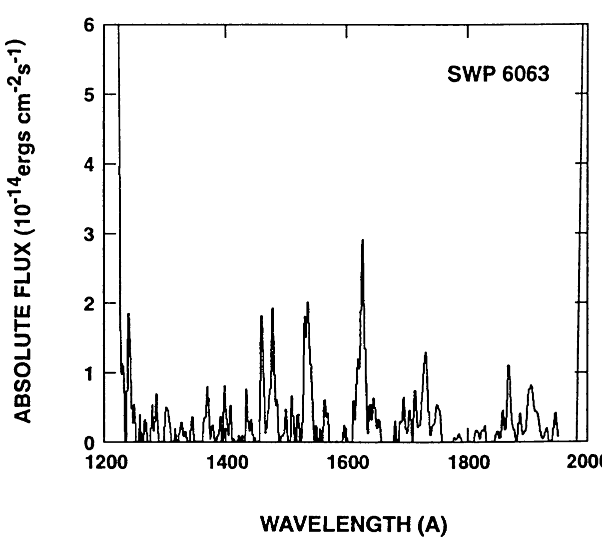

FIG. 20.—Low-resolution SWP observation of AS 295B taken in 1979 August. This spectrum exhibits broad emission lines from C IV and He II, superposed on a underexposed UV continuum.

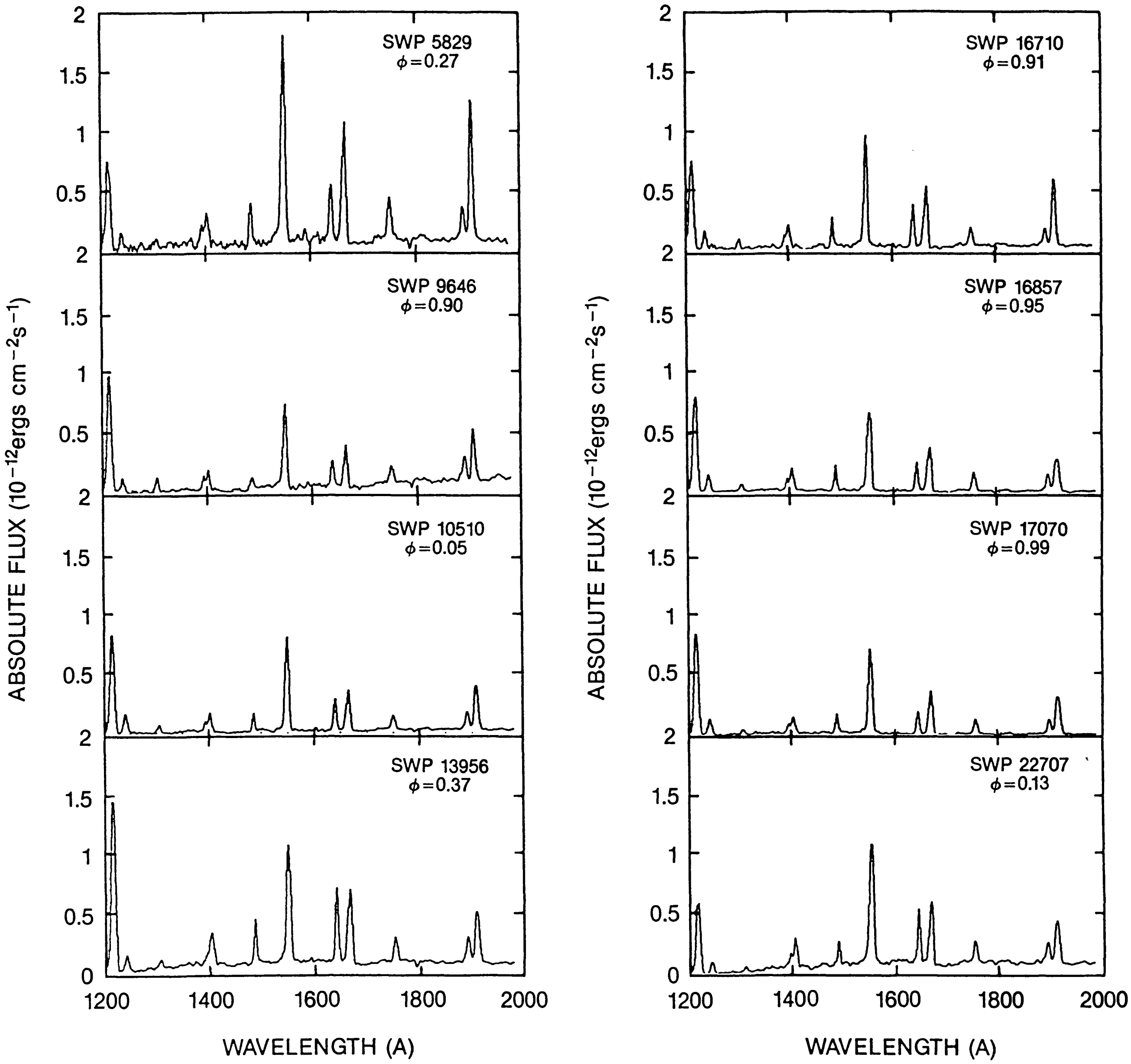

FIG. 21.—Low-resolution *IUE* spectra of AR Pavonis obtained in and out of eclipse. Orbital phases were determined from Andrews (1974) min (V) = 2,420,330 + 604.4^{d}E. Notice that the strength of the UV continuum flux distribution exhibits orbital phase dependence.

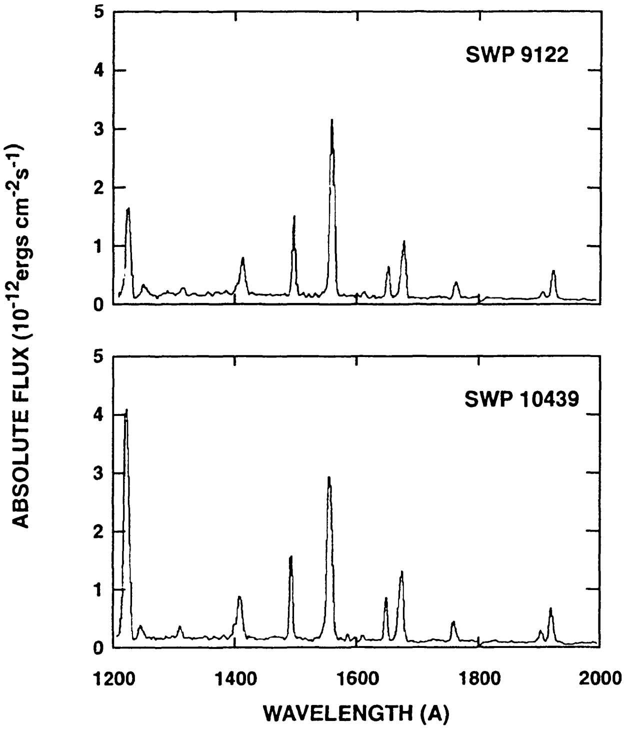

FIG. 22.—Low-resolution SWP spectra of V443 Herculis obtained in 1980. Both spectra exhibit a moderately strong UV continuum accompanied with many intense emission lines. C IV λλ 1548,1550 is particularly strong.

lines are very weak in most observations of BF Cyg, except SWP 28734 and SWP 33579, which are at about $\Phi = 0.7$. Spectra taken between 1986 July and 1988 May contain more emission lines shortward of 1500 Å than spectra obtained from 1979 June to 1981 March.

4.24. *CH Cygni*

The far-UV spectra of CH Cyg (Figure 24) show many variations covering the period 1979–1987. Usually, the continuum is rather flat, but rises with increasing wavelength during outburst. Several emission lines, e.g., O I λλ 1302–1306, C IV λλ 1548,1550, He II λ1640 and O III] λλ 1660,1666, are present with little sign of any absorption. However, some spectra (e.g., SWP 22056) have a continuum flux distribution that can be attributed to an opaque UV absorbing region dominated by multiplets of Fe II and other singly ionized metals. The UV continuum strength increased by a factor of 5 between 1979 December (SWP 7409) and 1984 January (SWP 22056) when CH Cyg underwent an outburst (Selvelli & Hack 1985), then decreased to about 20% of this value by 1985 January (SWP 24956). SWP 24956 exhibits many semiforbidden lines (e.g., N III], Si III], and C III]).

The UV continuum continued to decline until 1986 January (SWP 27571), when it again resembled its preoutburst state (e.g., SWP 7409) and singly ionized metallic absorption was evident. The most recent *IUE* spectrum of CH Cyg (SWP 30134), taken in 1987 January has a weak and flat continuum

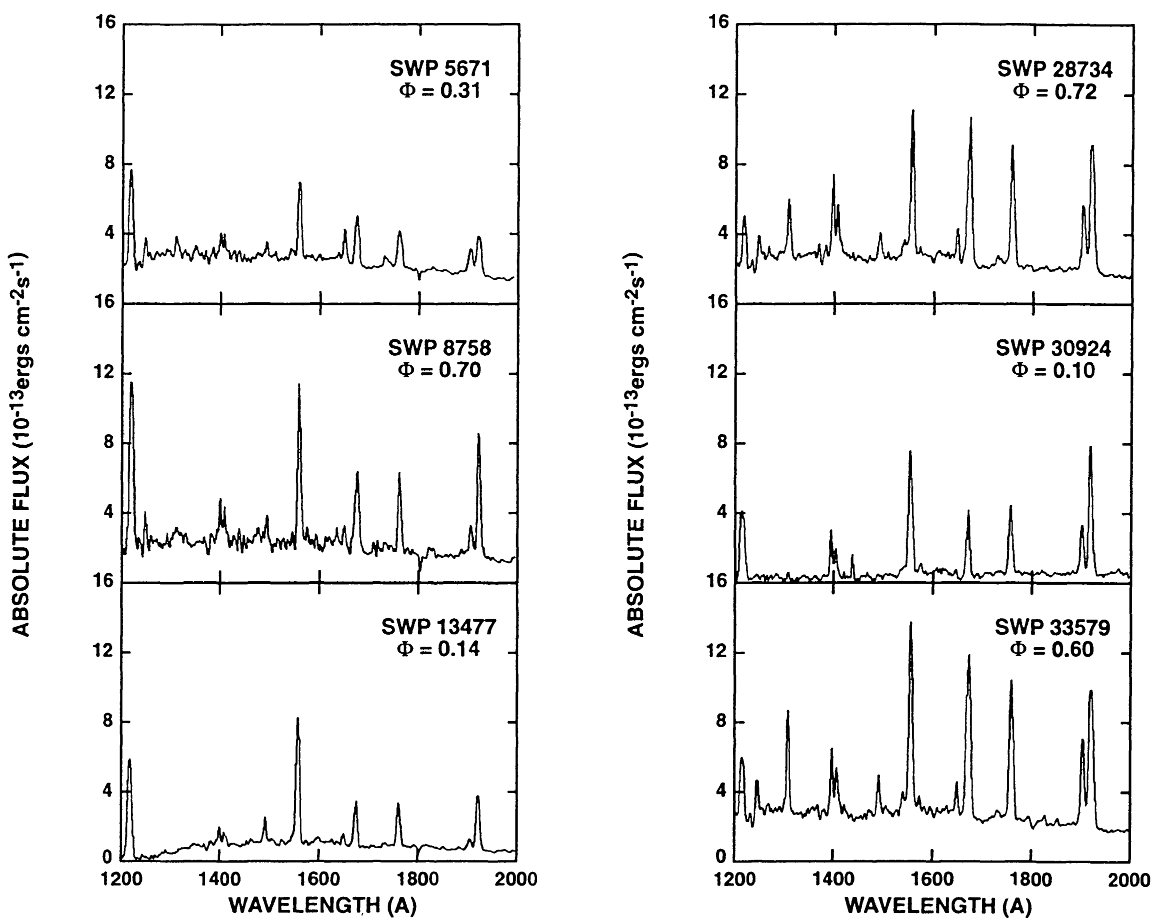

FIG. 23.—Low resolution *IUE* spectra of the symbiotic star BF Cygni. Near minimum the UV continuum flux decreases noticeably. Orbital phases were calculated using the ephemeris min(pg) = 2,415,058 + 756.8^{d}E (Mikolajewska 1987).

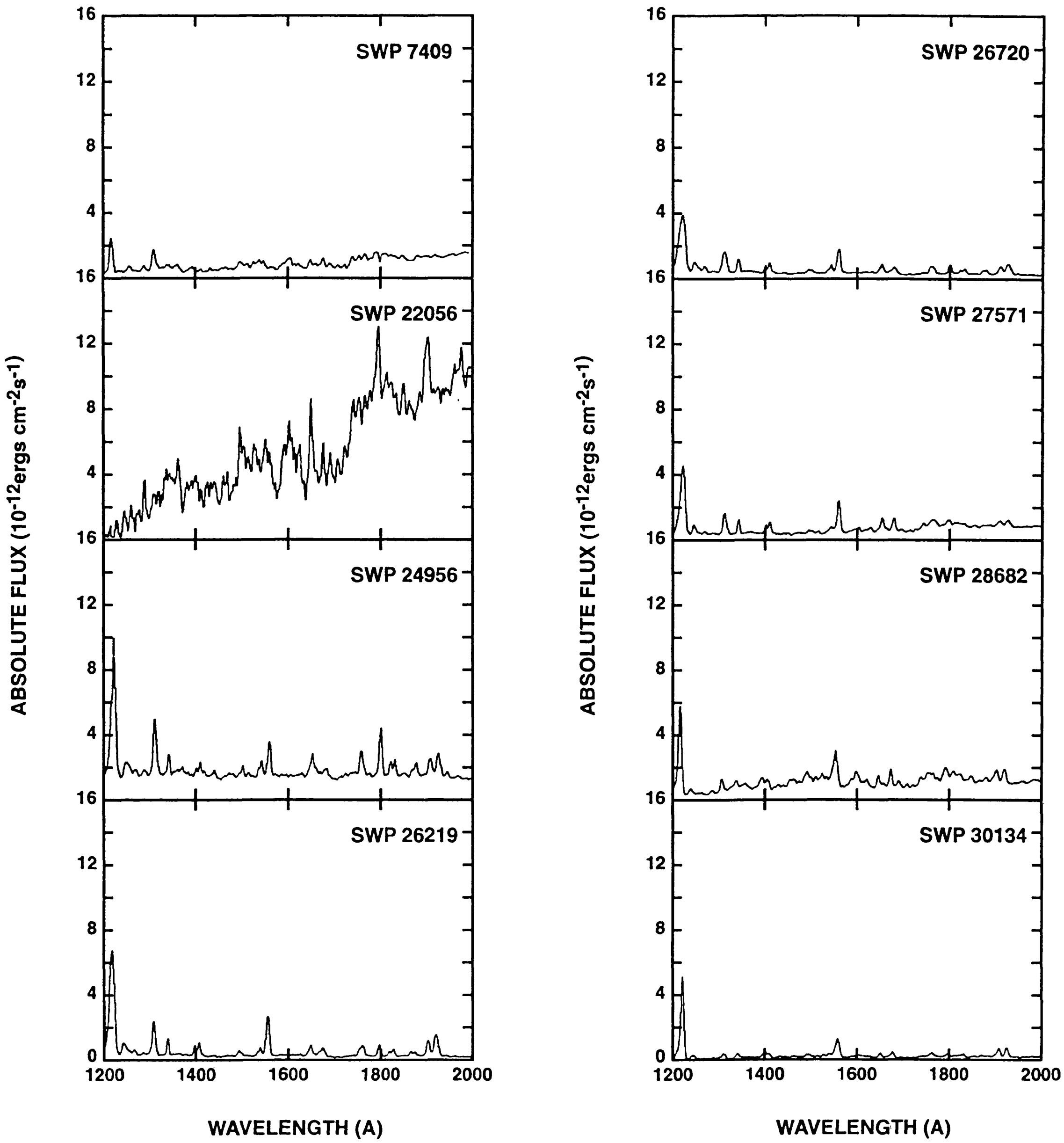

FIG. 24.—Low-resolution spectra of CH Cyg obtained from 1979 December to 1987 January. The continuum is highly variable in flux level and wavelength distribution. SWP 22056 was taken following outburst, when the UV continuum was heavily blanketed by Fe II absorption.

that is accompanied by weak emission features, suggesting that the system is in a low-excitation, quiescent state. Line blanketing from Fe II is not apparent.

4.25. *HM Sagittae*

The *IUE* spectra of the D-type symbiotic star HM Sge shown in Figure 25 are characterized by a very weak, flat continuum with many intense emission lines of N V, N IV], C IV, He II, O III], Si III], C III]. These spectra show that the emission-line intensities decreased slightly between 1980 August (SWP 9898) and 1981 August (SWP 14756) but increased by about a factor of 2 through 1982 April (SWP 16752) to 1986 August (SWP 28896). This activity was followed by a decrease from 1986 August to 1987 April.

4.26. *CI Cygni*

The far-UV spectra in Figure 26 show CI Cyg in and out of eclipse in 1980 and 1982. There are many prominent emission lines (e.g., N IV], C IV, He II, O III], and C III]) superposed on a flat continuum which disappears at visual minimum phase (Aller 1954). During the 1982 eclipse, many resonance lines such as N V and He II were stronger than during the 1980 eclipse. Many of the intersystem lines (e.g., O III], N III], C III]) were much brighter during the 1980 eclipse, suggesting the hot source interacted more with the M giant atmosphere than in 1982 during the earlier eclipse phase.

4.27. *V1016 Cygni*

The UV spectrum of V1016 Cyg displays many intense emission lines (N V, O I, O IV], N IV], C IV, He II, O III], N III], Si III], and C III]) superposed on a weak continuum. As shown in Figure 27, the emission lines [Ne V] λ1574 and [Ne IV] λ1601, usually weak in most symbiotics, are very strong in the UV spectrum of V1016 Cyg. All orbital phases were determined using the UV ephemeris of Nussbaumer & Schmid (1988). During a UV maximum, $\Phi = 0.5$ (± 0.1), the emission lines increase in strength by a factor of about 2. The strongest emission spectra reproduced are SWP 5611 and SWP 9878, both of which are near UV maximum. Whitelock (1987) finds that the UV continuum is strongly reduced by both interstellar and circumstellar reddening.

4.28. *RR Telescopii*

The SWP spectra shown in Figure 28 exhibit many strong emission lines that include N V, Si IV, O IV], N IV], C IV, He II, O III], and C III], reflecting a broad range of ionization energies. There are many strong permitted lines from the spectra of N V, C IV, and He II that provide evidence of a hot star $T_{\rm hot} \geq 10^5$ K. The emission-line intensities have varied by a factor of 2 or 3 between the 1978 and 1987 *IUE* observations, consistent with the behavior of slow novae which exhibit a slow decline following outburst.

4.29. *HBV 475*

The far-UV spectrum of HBV 475 (or V1329 Cyg) exhibits very weak UV continuum flux and a wide assortment of permitted and intersystem lines that includes N V, Si IV, O IV],

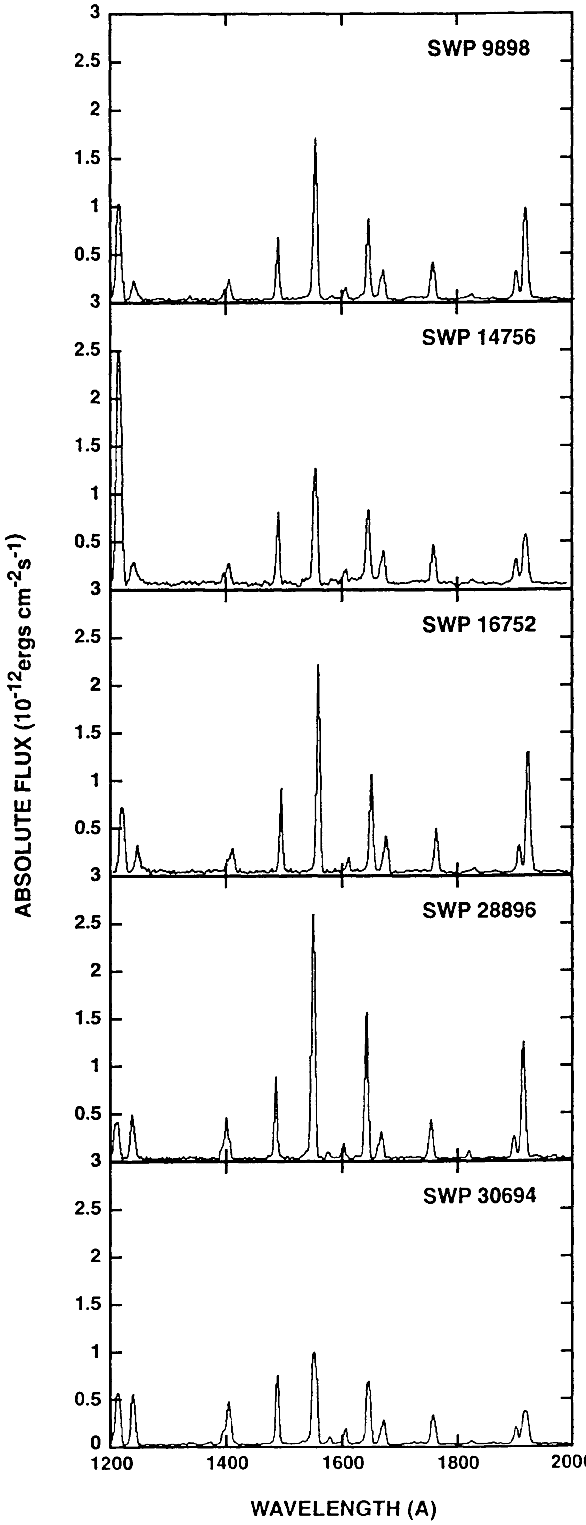

FIG. 25.—Low-resolution *IUE* spectra of HM Sagittae. This system exhibits many intense permitted and intersystem emission lines that are superposed on a flat UV continuum. C IV, He II, and C III] produce the strongest emission lines in the spectra.

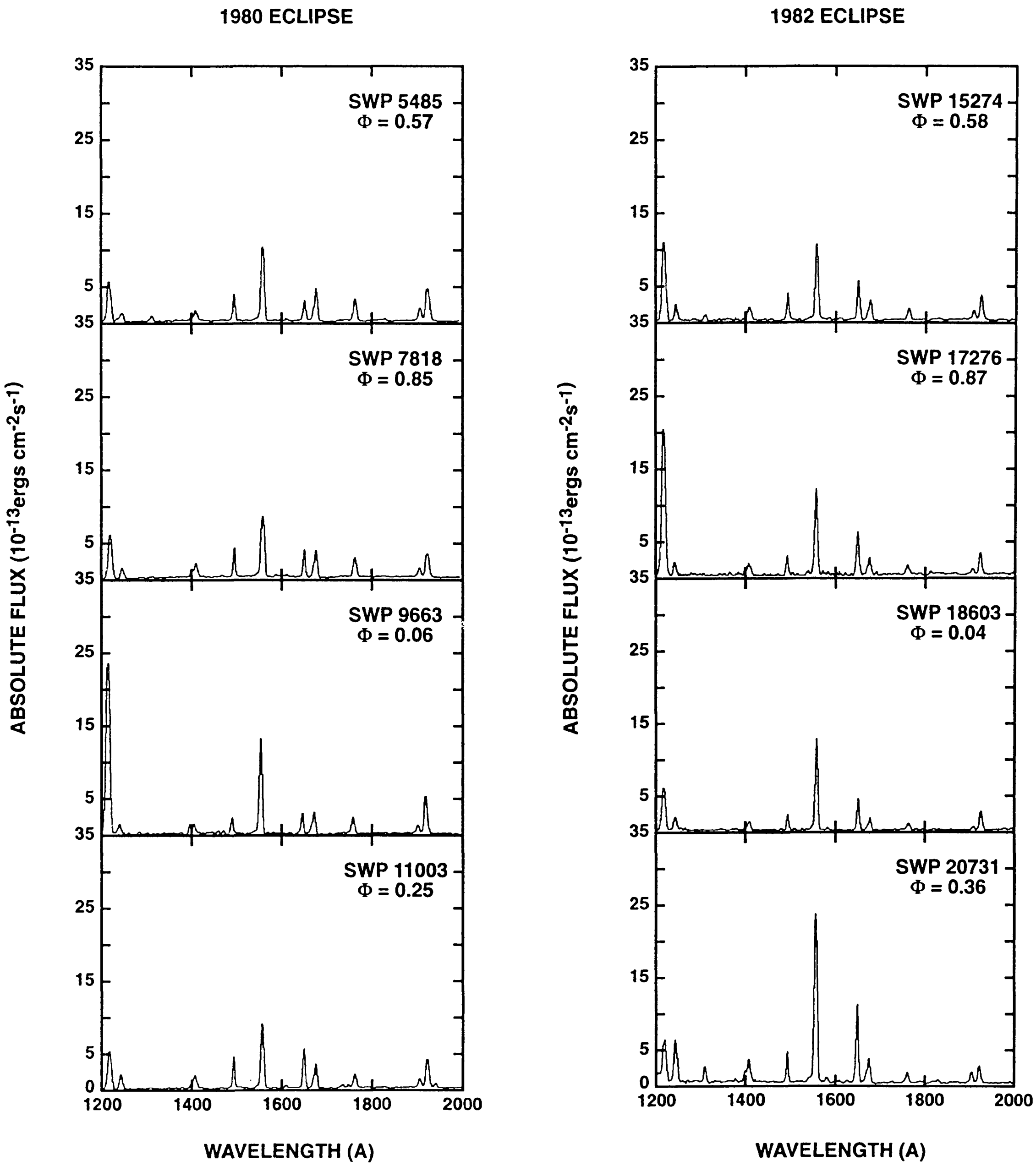

FIG. 26.—Low-resolution spectra of CI Cygni taken between 1979 June and 1983 August. These spectra were obtained before and after eclipses that occurred in 1980 July and 1982 November. During a minimum phase, $\Phi = 0.0\ (\pm 0.1)$, the UV continuum disappears, while at maximum, $\Phi = 0.5\ (\pm 0.1)$, the continuum is slightly elevated. Orbital phases for each spectrum were found from Aller (1954) min(V) = JD 2,411,902 + $855^{d}.25$.

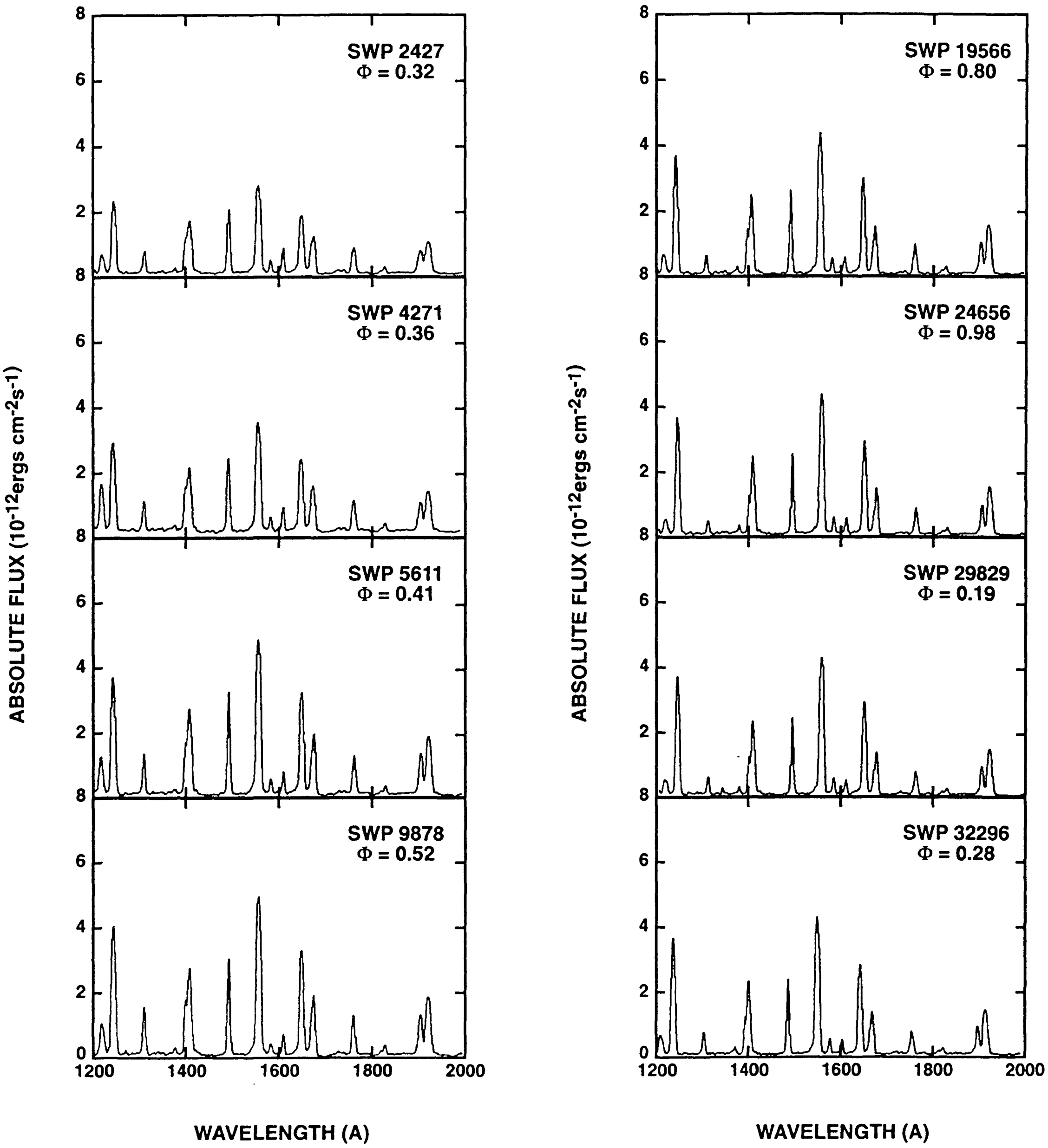

FIG. 27.—Low-resolution spectra of V1016 Cygni obtained between 1978 August and 1987 November. V1016 Cygni exhibits many broad, permitted, and intersystem emission lines. Orbital phases were determined from Nussbaumer & Schmid (1988) min(UV) = JD 2,444,101 + 3470$^d E$.

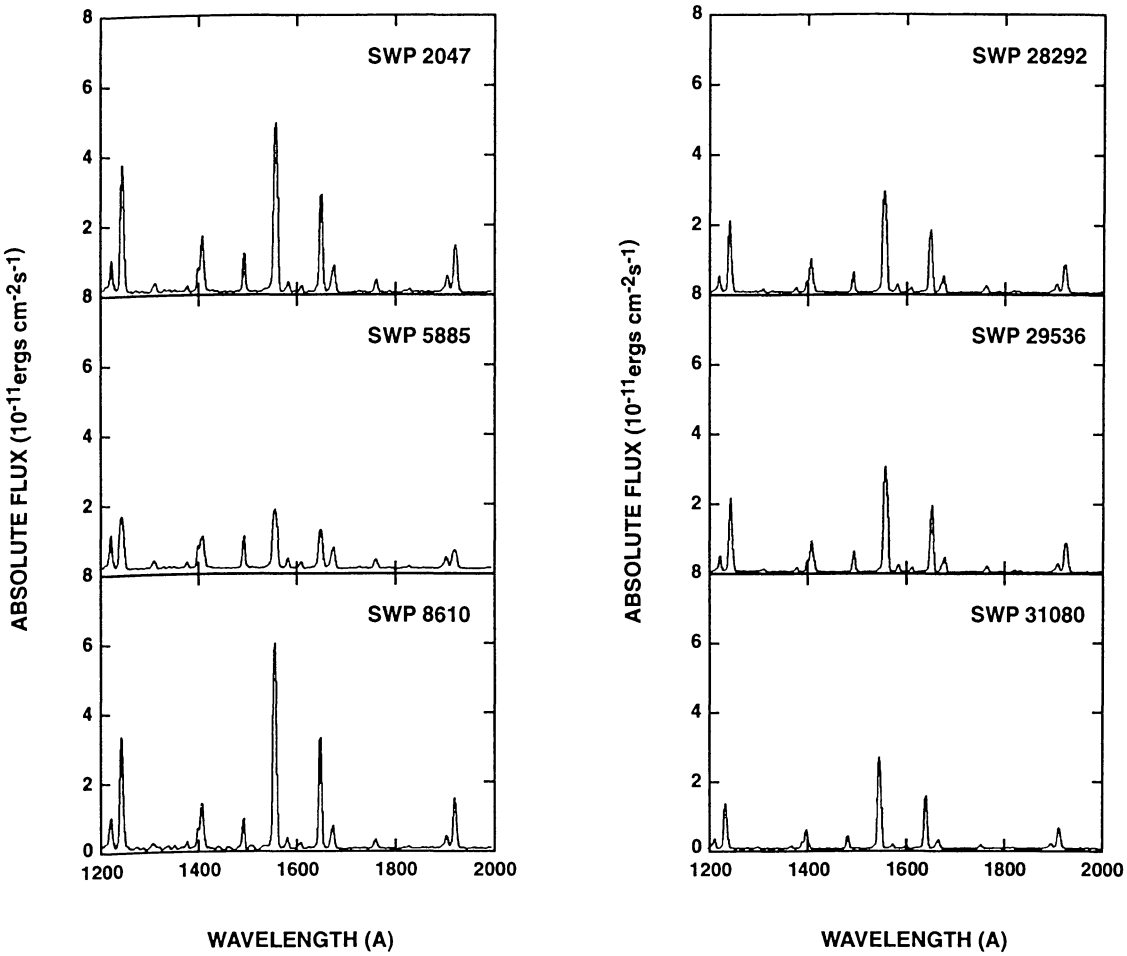

FIG. 28.—Low-resolution SWP spectrum of RR Telescopii. This spectrum contains numerous high-excitation emission lines, the most intense are N V, C IV and He II. The UV continuum flux is relatively flat and independent of wavelength.

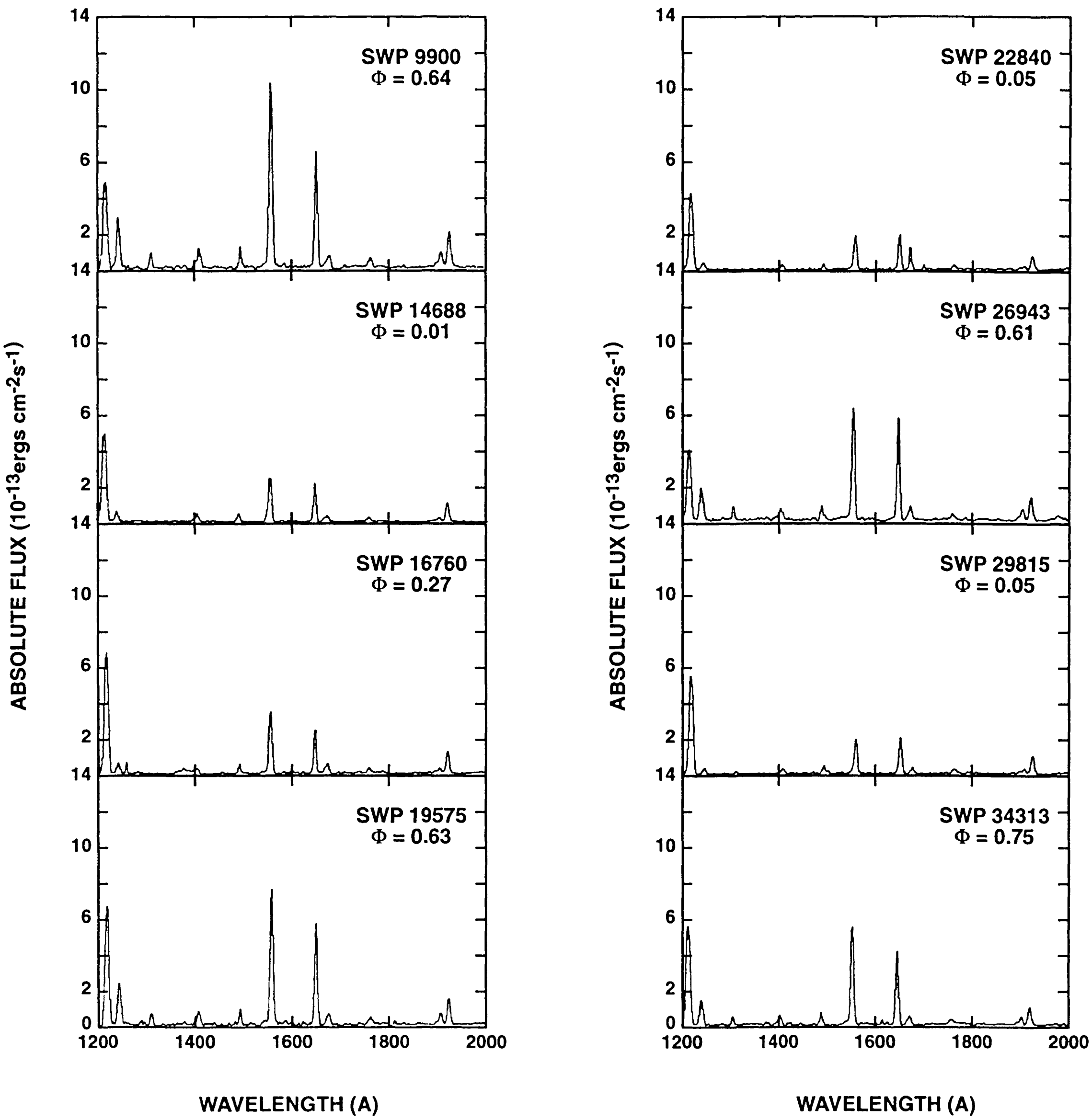

FIG. 29.—Low-resolution *IUE* spectra of HBV 475 (=V1329 Cyg) obtained between 1980 August to 1988 September. Emission line intensities increase near maxima $\Phi = 0.5\ (\pm 0.1)$ and decrease near minima $\Phi = 0.0\ (\pm 0.1)$. The orbital ephemeris min (V) = JD 2,424,870 + $950^{d}E$ was derived by Grygar et al. (1979).

C IV, He II, O III], N III], Si III], and C III]. The permitted lines are much stronger in absolute flux than the intersystem lines (Fig. 29). *IUE* spectra taken between 1980–1988 show increased emission during a visual maximum phase $\Phi = 0.5$ (± 0.1) and a subsequent decrease in activity during a visual minimum $\Phi = 0.0$ (± 0.1). Orbital phase values were calculated using the ephemeris min(V) = JD 2,424,870 + $950^{d}E$ (Grygar et al. 1979). There is a decrease in most emission-line intensities by a factor of 3, 4, or even greater between phase $\Phi = 0.5$ (± 0.1) and phase $\Phi = 0.0$ (± 0.1). During minima, both the UV continuum and emission lines have decreased intensity, providing evidence of an eclipsing binary system.

4.30. *AG Pegasi*

AG Peg is one of the brightest symbiotic stars in the SWP wavelength range. The UV spectrum contains many broad intense emission lines (e.g., N V, N IV], C IV, He II, and O III]) and a UV continuum which rises toward shorter wavelengths. In Figure 30, N V λλ 1238,1242 has a broad base, perhaps in part due to continuum flux. The rise of continuum emission with decreasing wavelength indicates a hot component with $T_{\rm hot} \geq 10^5$ K; many authors have determined $30{,}000 \leq T_{\rm hot} \leq 100{,}000$ K (Gallagher et al. 1979; Keyes & Plavec 1980; Kenyon & Webbink 1984). N IV] λ1487 is exceptionally strong, while the semiforbidden line intensities of N III] λλ 1747–1753, Si III] λ1892, and C III] λλ 1907,1909 longward of 1700 Å are weak (Fig. 30), suggesting a very dense ($n_e \geq 10^{10}$ cm^{-3}) nebular region (Keyes & Plavec 1980; Penston & Allen 1985).

4.31. *Z Andromedae*

The far-UV spectrum of Z And shows many strong intercombination and permitted emission lines that are superposed on a strong continuum which increases toward longer wavelengths during activity but is relatively flat in quiescence. Figure 31 presents eight SWP spectra taken between the years 1978 to 1988. The system was in a quiescent state between 1978 April (SWP 5809) to 1984 March (SWP 11006). An outburst occurred in 1984 March that preceded a larger outburst in 1985 September to 1986 May (SWP 26937, 27028, 27203, 27632), which was followed by a period of quiescence from 1986 June to 1988 January (SWP 32208, 32845) (Cassatella et al. 1988a,b). In outburst, there was an increase in UV absolute continuum flux that was accompanied by an increase in emission line intensities by factors of 2 or 3 for many of the intersystem lines (e.g., O III], N III], Si III] and C III]) that become more pronounced in outburst.

The continuum rises with longer wavelengths, suggesting that the hot source is photoionizing material from the cool

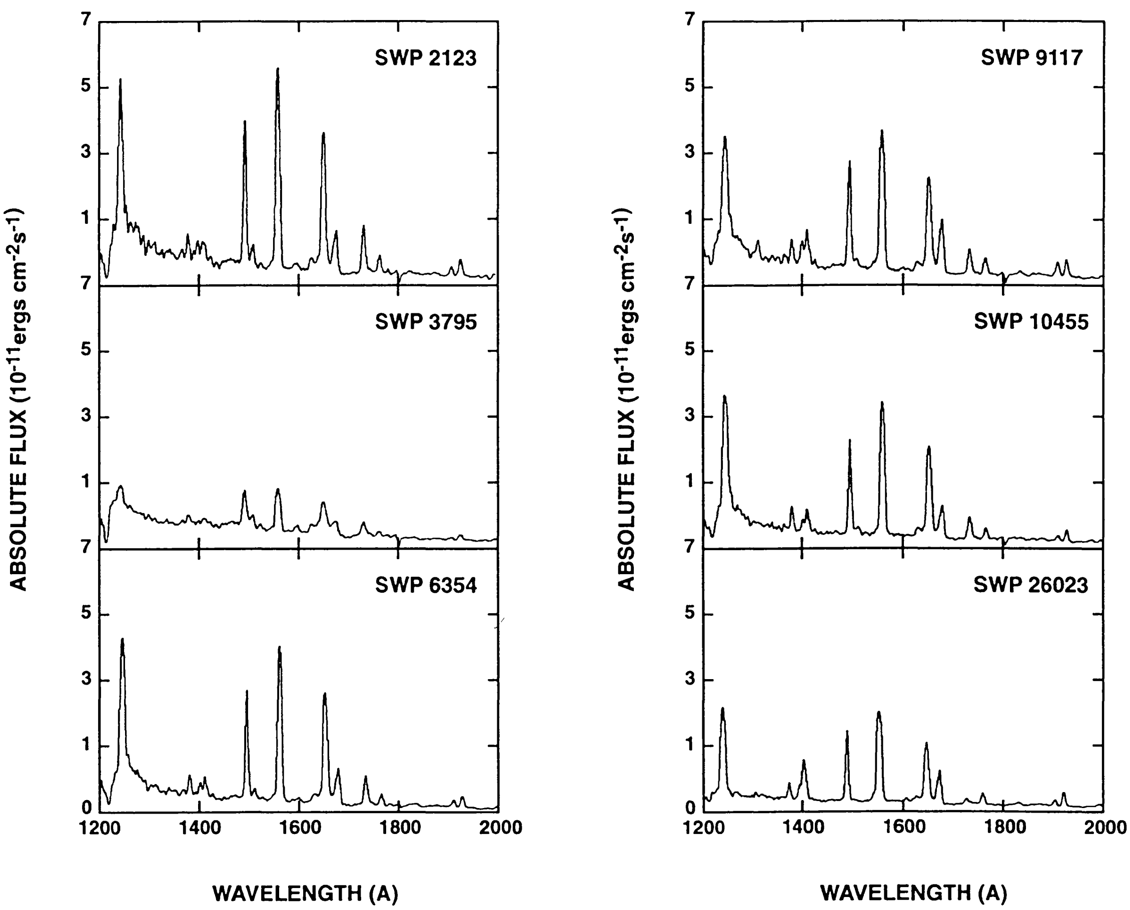

FIG. 30.—Low-resolution spectra of AG Pegasis. Many prominent resonance emission lines (e.g., N V, C IV, and He II) dominate the far-UV. Note the UV continuum flux distribution increase toward shorter wavelengths consistent with a hot subdwarf.

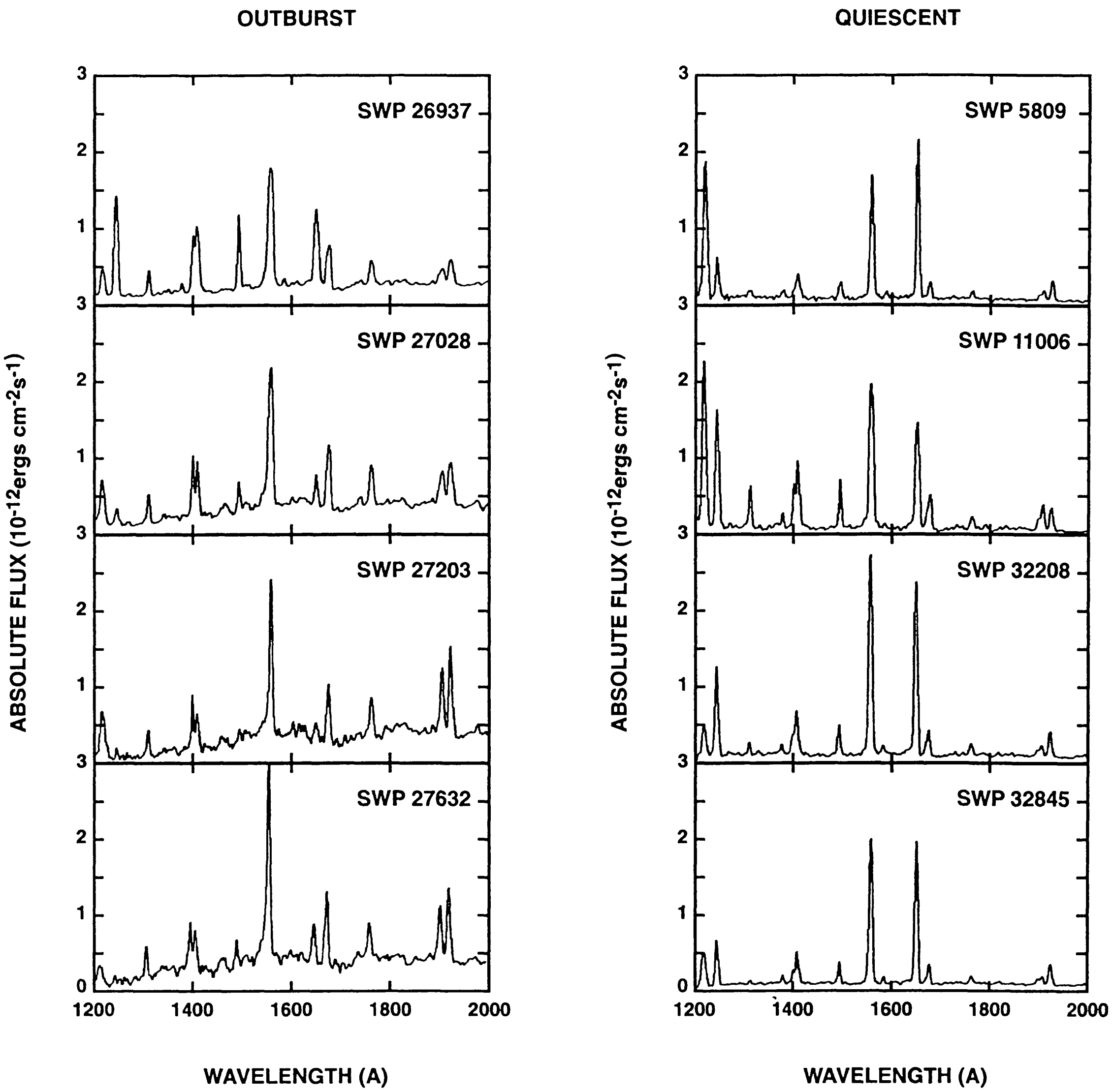

FIG. 31.—Low-resolution spectra of Z Andromedae obtained during outburst and quiescent phases. In quiescence, the spectra exhibit a flat UV continuum with strong permitted lines of C IV λλ 1548,1550 and He II λ1640. During outburst, the intersystem emission lines dominate the spectrum, while the UV continuum rises noticeably toward longer wavelengths.

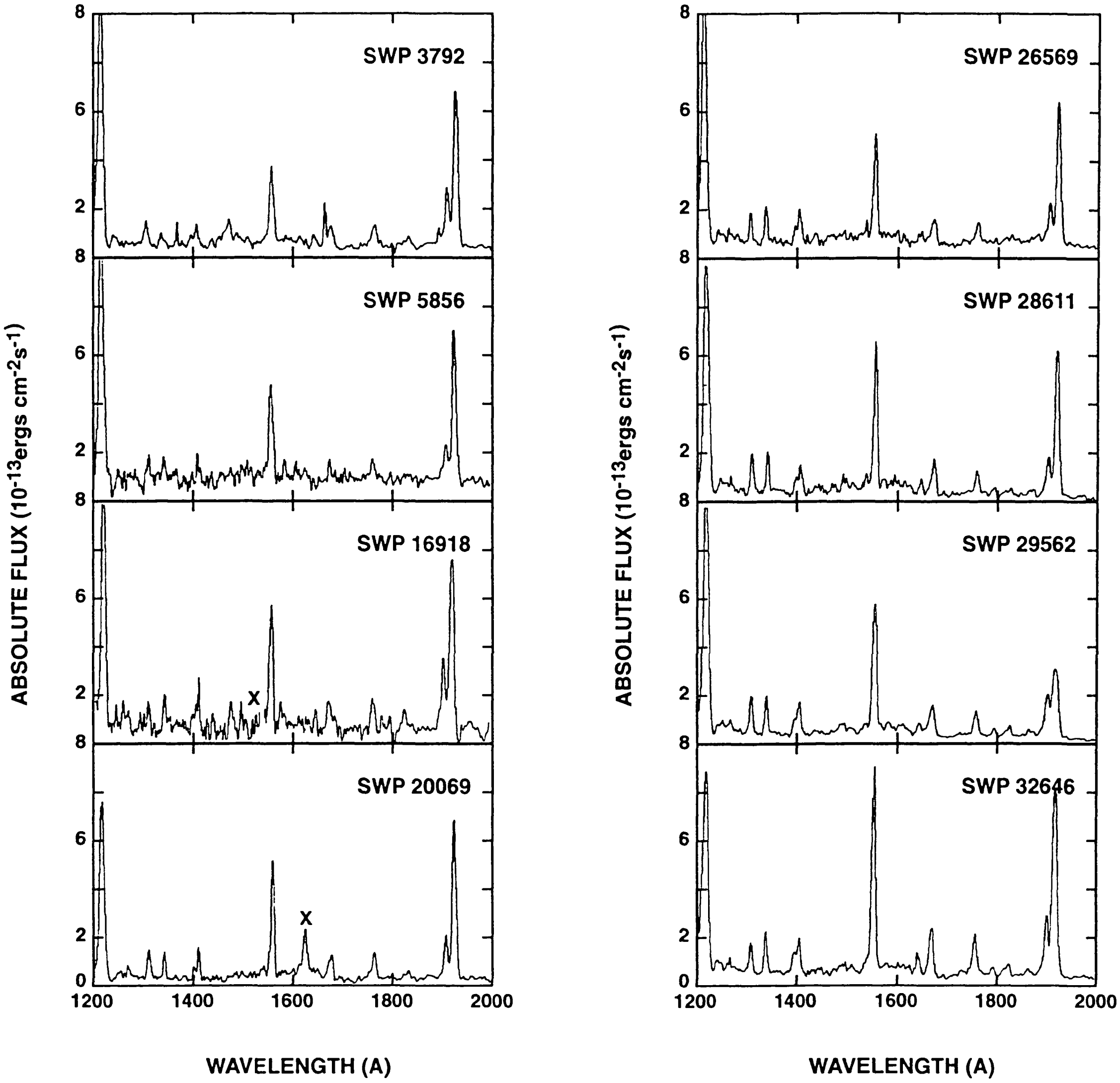

FIG. 32.—Low-resolution *IUE* spectra of the H II region of R Aquarii, obtained between 1979 January and 1988 January. The spectra show a few intense emission lines (e.g., C IV and C III]) and a moderately strong continuum. An X signifies a cosmic ray hit.

component. This behavior agrees with the model of Fernandez-Castro et al. (1988). During quiescence, the UV continuum is relatively flat and the permitted emission lines of N V, C IV, and He II are much brighter than during outburst, indicating that the photoionizing flux emitted by the hot star is enhanced.

4.32. *R Aquarii*

R Aqr is a complex, D-type system containing a cool Mira, a hot secondary, a circumstellar envelope, and a jet of nebular material extending ~6" NE of the system (Wallerstein & Greenstein 1980). The *IUE* observations of the H II region of R Aqr shown in Figure 32 reveal moderate emission lines such as C IV λλ 1548,1550, O III] λλ 1660,1666, N III] λλ 1747–1753, Si III] λ1892 and C III] λλ 1907,1909. SWP spectra taken between 1979 January and 1988 January reveal weak to moderate emission strength, with C IV and C III] being the strongest lines. The continuum flux distribution is relatively flat as a function of wavelength over the entire SWP range.

REFERENCES

Allen, D. A. 1981, MNRAS, 197, 739
———. 1982, IAU Colloq. 70, Nature of Symbiotic Stars, ed. M. Friedjung & R. Viotti (Dordrecht: Reidel), 27
———. 1984, Proc. Astron. Soc. Australia, 5 (3), 369
Aller, L. H. 1954, Publ. Dom. Astrophys. Obs. Victoria, 9, 321
Anderson, C. M., Cassinelli, J. P., & Sanders, W. T. 1981, ApJ, 247, L127
Andrews, R. G. 1974, MNRAS, 167, 635
Bohlin, R. C., & Grillmair, C. J. 1988, ApJ, 66, 209
Boyarchuk, A. A. 1975, IAU Symp. 67, Variable Stars and Stellar Evolution, ed. V. E. Sherwood & L. Plaut (Dordrecht: Reidel), 377
Cassatella, A., Fernandez-Castro, T., & Oliversen, N. A. 1988a, in The Symbiotic Phenomenon, ed. J. Mikolajewska et al. (Dordrecht: Kluwer), 181

Cassatella, A., Gonzalez-Riestra, R., Fernandez-Castro, T., Fuensalida, J., & Gimenez, A. 1988b, in The Symbiotic Phenomenon, ed. J. Mikolajewska et al. (Dordrecht: Kluwer), 301
Chochol, D., Skopal, A., Vittone, A., & Mammano, A. 1987, Ap & SS, 131, 758
Fernandez-Castro, T., Cassatella, A., Gimenez, A., & Viotti, R. 1988, ApJ, 324, 1016
Gallagher, J. S., Holm, A. V., Anderson, C. M., & Webbink, R. F. 1979, ApJ, 229, 994
Grygar, J., Hric, L., Chochol, D., & Mammano, A. 1979, Bull. Astron. Inst. Czechoslovakia, 30, 8
Guitierrez-Moreno, A., Moreno, H., & Cortes, G. 1986, A & A, 166, 143
Kafatos, M., Michalitsianos, A. G., Allen, D. A., & Stencel, R. E. 1983, ApJ, 275, 584
Kafatos, M., Michalitsianos, A. G., & Feibelman, W. A. 1982, ApJ, 257, 204
Kafatos, M., Michalitsianos, A. G., & Hobbs, R. W. 1980, ApJ, 240, 114
Kafatos, M., Meier, S. R., & Martin, I. 1993, ApJS, 84, 201
Kenyon, S. J. 1982, PASP, 94, 165
———. 1986, The Symbiotic Stars (Cambridge: Cambridge Univ. Press)
Kenyon, S. J., & Bateson, F. M. 1984, PASP, 96, 321
Kenyon, S. J., & Fernandez-Castro, T. 1987, AJ, 93, 938
Kenyon, S. J., & Garcia, M. R. 1986, AJ, 91, 125
Kenyon, S. J., & Webbink, R. F. 1984, ApJ, 279, 252
Keyes, C. D., & Plavec, M. J. 1980, in The Universe at Ultraviolet Wavelengths, ed. R. Chapman (NASA CP-2171), 443
Michalitsianos, A. G., Kafatos, M., Feibelman, W. A., & Wallerstein, G. 1982, A & A, 109, 136
Mikolajewska, J. 1987, Ap & SS, 131, 713
Munari, U. 1988, IAU Circ., No. 4622
Munari, U., Margoni, R., Iijima, T., & Mammano, A. 1988, A & A, 198, 173
Nussbaumer, H., & Schmid, H. M. 1988, A & A, 192, L10
Penston, M. V., & Allen, D. A. 1985, MNRAS, 212, 939
Penston, M. V., et al. 1983, MNRAS, 202, 833
Sahade, J., Brandi, E., & Fontenla, J. M. 1984, A & AS, 56, 17
Schulte-Ladbeck, R. 1988, A & A, 189, 97
Seaquist, E. R. 1988, in The Symbiotic Phenomenon, ed. J. Mikolajewska et al. (Dordrecht: Kluwer), 69
Seaquist, E. R., & Taylor, A. R. 1990, ApJ, 349, 313
Selvelli, P. L., & Hack, M. 1985, Astron. Express, 1(4–6), 115
Swings, J. P., & Allen, D. A. 1972, PASP, 84, 523
Viotti, R. 1993, in Cataclysmic Variables and Related Objects, ed. M. Hack & C. la Dous (NASA SP-507), 634
Viotti, R., Piro, L., Friedjung, M., & Cassatella, A. 1987, ApJ, 319, L7
Wallerstein, G., & Greenstein, J. L. 1980, PASP, 92, 275
Whitelock, P. A. 1987, PASP, 99, 573